JOURNAL OF GEOPHYSICAL RESEARCH, VOL. 105, NO. E2, PAGES 4135–4152, FEBRUARY 25, 2000

Structures in tessera terrain, Venus: Issues and answers

Vicki L. Hansen,[1] Roger J. Phillips,[2] James J. Willis,[3] and Rebecca R. Ghent[1]

Abstract. Many workers assume that tessera terrain, marked by multiple tectonic lineaments and exposed in crustal plateaus, comprises a global onionskin on Venus. Because tesserae are exposed mostly within crustal plateaus, which exhibit thickened crust, issues of tessera distribution and the mechanism of crustal plateau formation (e.g., mantle downwelling or upwelling) are intimately related. A review of Magellan data indicates that tessera terrain does not form a global onionskin on Venus, although ribbon-bearing tesserae reflect an ancient time of a globally thin lithosphere. Individual tracts of ribbon-bearing tessera terrain formed diachronously, punctuating time and space as individual deep mantle plumes imparted a distinctive rheological and structural signature on ancient thin crust across spatially discrete 1600-2500 km diameter regions above hot mantle plumes. Plume-related magmatic accretion led to crustal thickening at these locations, resulting in crustal plateaus. Crustal plateau surfaces record widespread early extension (ribbon structures) and local, minor perpendicular contraction of a thin, competent layer above a ductile substrate. Within individual evolving crustal plateaus the thickness of the competent layer increased with time, and broad, gentle folds formed along plateau margins and short, variably oriented folds formed in the interior; late complex graben cut folds. Local lava flows accompanied all stages of surface deformation. In contrast to these conclusions, *Gilmore et al.* [1998] summarized post-Magellan arguments in favor of downwelling models for crustal plateau formation. In light of this discrepancy, we reexamine the regions investigated by these workers and evaluate their arguments against upwelling models. We show that *Gilmore et al.* [1998] did not differentiate ribbons from graben and therefore their proposed temporal relations are invalid; they disregarded shear fracture ribbons, thus invalidating their criticism of ribbon models; they misunderstood previous radargrammetric work that constrains ribbon geometry; and they relied solely on geometrical relations to constrain timing, violating kinematic analysis methodology. Their stratigraphic constraints on ribbon-fold temporal relations are invalid because they (1) misinterpreted implications of map relations; (2) did not isolate radar artifacts due to local radar slope effects from proposed material units; (3) chose a region for analysis that clearly shows the effects of younger tectonism and volcanism; and (4) presented map relations that cannot be reproduced. Their attempts to discount upwelling models of crustal plateau formation fail because they combine fundamentally different pre-Magellan and post-Magellan upwelling models. These misconceptions about the upwelling model and processes responsible for global warming [*Phillips and Hansen*, 1998], lead to serious errors in *Gilmore et al.*'s [1998] criticism. Furthermore, we show that the data of *Gilmore et al.* [1998] are actually more consistent with upwelling than downwelling models, consistent with arguments that tessera terrain is not global in spatial distribution.

1. Introduction

Tessera terrain, characterized by intersecting suites of tectonic lineaments, high relief relative to surroundings, and high surface roughness [*Basilevsky et al.*, 1986], comprises 8-10% of Venus' surface. Many workers assume that tessera terrain forms a globally extensive layer that extends almost everywhere beneath the regional plains [e.g., *Solomon*, 1993; *Turcotte*, 1993; *Grimm*, 1994a; *Herrick*, 1994; *Ivanov and Head*, 1996; *Nimmo and McKenzie*, 1998; *Basilevsky and Head*, 1998; *Head and Basilevsky*, 1998]. Although a global onionskin of tessera would simplify global stratigraphic studies and provide important constraints for geodynamical models, such an assumption is unwarranted, as several distinct types of tessera terrain exist and record distinct mechanisms of formation [e.g., *Hansen and Willis*, 1996]. Ribbon-bearing tesserae characterize crustal plateaus (Fortuna, Tellus, Alpha, eastern Ovda, western Ovda, Phoebe and Thetis), steep-sided, flat-topped, quasi-circular regions ~1600 to 2500 km in diameter (Figure 1). Ribbon-bearing tessera terrain is also preserved locally in large arcuate tessera inliers, postulated to be collapsed crustal plateaus [*Phillips and Hansen*, 1994; *Hansen et al.*, 1997]. Many workers agree that thickened crust supports crustal plateaus, as evidenced by small gravity anomalies, low gravity to topography ratios, shallow apparent depths of compensation, and consistent admittance spectra [*Smrekar and Phillips*, 1991; *Bindschadler et al.*,

[1]Department of Geological Sciences, Southern Methodist University, Dallas, Texas.
[2]Department of Earth and Planetary Sciences, Washington University, St. Louis, Missouri.
[3]Department of Geology, University of Louisiana at Lafayette.

Paper number 1999JE001137.
0148-0227/00/1999JE001137$09.00

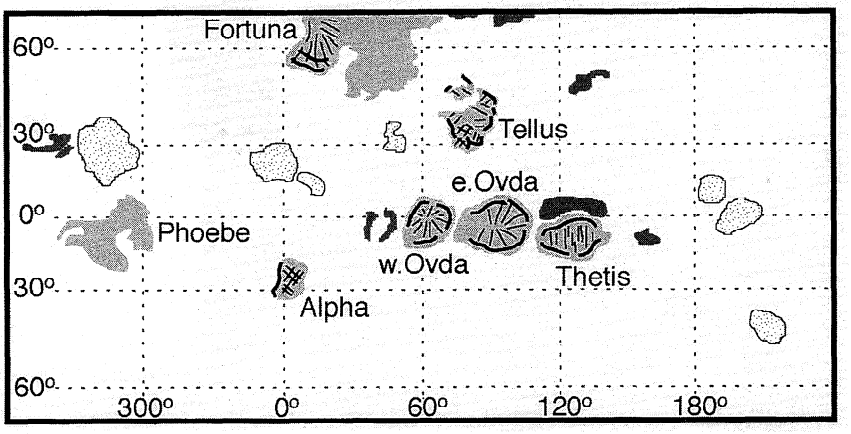

Figure 1. Venus: volcanic rises (stipple), large tessera inliers (dark), and crustal plateaus (light shading) with fold (thick lines) and ribbon (thin lines) trends (trends from *Bindschadler et al.* [1992a and b], *Pritchard et al.* [1997], and *Ghent and Hansen* [1999]).

1992a,b; *Grimm*, 1994b; *Simons et al.*, 1997], but disagree about the thickening mechanism. Debates surrounding tessera and crustal plateau formation have centered about a few major questions, the answers to which become underlying assumptions in geodynamic models (Table 1). For example, is tessera terrain global in distribution and globally synchronous in formation or localized in space and time at individual crustal plateaus? Is thick crust at crustal plateaus the result of subsolidus crustal flow related to mantle downwelling, or is thick crust the result of magmatic processes related to mantle upwelling? These issues have implications for how convection in the Venusian mantle interacts with the lithosphere in time and space, and how both the upper and lower thermal boundary layers of the convection system affect surface tectonics and volcanism. Because tessera are exposed mostly within crustal plateaus, issues of tessera distribution and the mechanism of crustal plateau formation are intimately related: did tessera formation predate, postdate, or accompany crustal thickening associated with crustal plateau formation? The tectonic and magmatic history of tesserae across crustal plateaus provides constraints for these questions.

Much of the crustal plateau debate was published prior to the Magellan mission or early during data return. Several years after Magellan it is valuable to revisit these questions in light of intervening analyses. Upwelling models of crustal plateau formation proposed prior to Magellan [*Herrick and Phillips*, 1990; *Phillips et al.*, 1991] postulated that volcanic rises evolved into crustal plateaus—a sequence not supported by Magellan data (see reviews by *Phillips and Hansen* [1994], *Bindschadler* [1995], and *Hansen et al.* [1997]). However, recognition of ribbon terrain, an extensional tectonic fabric that characterizes all crustal plateaus except Phoebe Regio [*Hansen and Willis*, 1996], led to the emergence of a new hotspot model [e.g., *Hansen et al.*, 1997; *Hansen and Willis*, 1998; *Phillips and Hansen*, 1998] in which crustal plateaus represent the signature of local mantle upwellings on ancient thin lithosphere, whereas volcanic rises represent the surface signature of local mantle upwellings on contemporary, relatively thick, lithosphere.

Gilmore et al. [1998] summarized the post-Magellan arguments in favor of mantle downwelling models, and against mantle upwelling models, for crustal plateau formation. Although tessera spatial distribution is a related issue, it was not addressed by these workers. *Gilmore et al.* [1998] attempted to disprove the geometric and kinematic analysis of ribbon formation and implications for crustal plateau

Table 1. Critical Questions With Regard to Tesserae and Crustal Plateau Formation and Suggested Solutions That Form Underlying Assumptions in Geodynamic Models

Question	Answer 1	Answer 2
What is the global 3D distribution of tesserae?	Tessera terrain is present globally under the plains, representing essentially global tessera formation (1, 12, 13, 14, 15, 17, 18).	Tessera terrain is localized in discrete regions—the regions of which may display broad global distribution (6, 9, 10, 11, 15).
What strain histories do tesserae record?	Extensional strain only postdates contractional strain (3, 4, 5, 7, 8, 13, 14, 15, 18).	Extensional strain predates *and* postdates contractional strain (6, 9, 10, 11, 16).
What is the timing of tessera formation?	Tessera terrain formed essentially throughout Venus' history (3, 4, 18).	Tessera terrain formed only relatively early in Venus' history (1, 11, 12, 13, 14, 15, 16, 17)
Did crustal plateaus form above mantle downwellings or upwellings?	Mantle downwelling (2, 3, 4, 5, 7, 8, 14, 17).	Mantle upwelling (6, 10, 11, 16).

1, *Basilevsky and Head* [1998]; 2, *Bindschadler and Parmentier* [1990]; 3, *Bindschadler et al.* [1992a]; 4, *Bindschadler et al.* [1992b]; 5, *Bindschadler* [1995]; 6, *Ghent and Hansen* [1999]; 7, *Gilmore et al* [1997]; 8, *Gilmore et al.* [1998]; 9, *Hansen and Willis* [1996]; 10, *Hansen et al.* [1997]; 11, *Hansen and Willis* [1998]; 12, *Head and Basilevsky* [1999]; 13, *Herrick* [1994]; 14, *Ivanov and Head* [1996]; 15, *Nimmo and McKenzie* [1998]; 16, *Phillips and Hansen* [1998]; 17, *Solomon* [1993]; 18, *Turcotte* [1993].

formation presented by *Hansen and Willis* [1996, 1998], as well as studies that build on those interpretations including structural analysis of southwestern Fortuna Tessera [*Pritchard et al.,* 1997], structural and kinematic analysis of eastern Ovda Regio [*Ghent and Hansen,* 1999], and further modeling of crustal plateau formation with implications for a global geodynamical model of Venus evolution [*Phillips and Hansen,* 1998]. We examine the arguments presented by *Gilmore et al.* [1998] and show that data from *Gilmore et al.'s* [1998] study areas instead support formation of tesserae above ancient, globally localized, mantle upwellings.

Gilmore et al. [1998] dispute the geometric and morphologic characterization of tessera structures, the temporal relations among tessera structures, and the resulting upwelling models [*Hansen and Willis,* 1996, 1998; *Pritchard et al.,* 1997; *Phillips and Hansen,* 1998; *Ghent and Hansen,* 1999]. We show that their analysis is in error on the basis of eight general issues.

1. *Gilmore et al.* [1998] did not differentiate ribbons from graben and therefore they cannot robustly address temporal relations between tessera structures.

2. They disregarded the documented distinction between tensile and shear fracture ribbons, thus invalidating their criticism of ribbon models.

3. They misunderstood radargrammetric work that constrains ribbon geometry [*Hansen and Willis*, 1996, 1998].

4. They propose ribbon-fold temporal relations based solely on geometry, a violation of kinematic analysis.

5. The constraints they term "stratigraphic" for ribbon-fold timing are invalid because they (1) misinterpreted implications of map relations; (2) did not isolate radar artifacts due to local radar slope effects from proposed material units and thus cannot uniquely identify material units; (3) chose a region for analysis that clearly shows the effects of younger tectonism and volcanism and thus obscures ribbon-fold relations; and (4) presented map relations that cannot be reproduced.

6. They did not differentiate between fundamentally different pre-Magellan and post-Magellan upwelling models, leading to mixed and matched assumptions among different models.

7. They misinterpreted the upwelling model of *Phillips and Hansen* [1998] with regard to (1) crustal annealing processes, (2) timing of ribbon formation relative to annealing processes, and (3) implications of annealing for pre-existing craters.

8. They misinterpret the volcanic mechanism proposed by *Phillips and Hansen* [1998] as responsible for global warming. In the following sections we use the techniques of structural and kinematic analysis to reexamine *Gilmore et al.*'s [1998] arguments and map areas, and we present new geologic mapping and thermal modeling results and discuss implications for the upwelling versus downwelling debate.

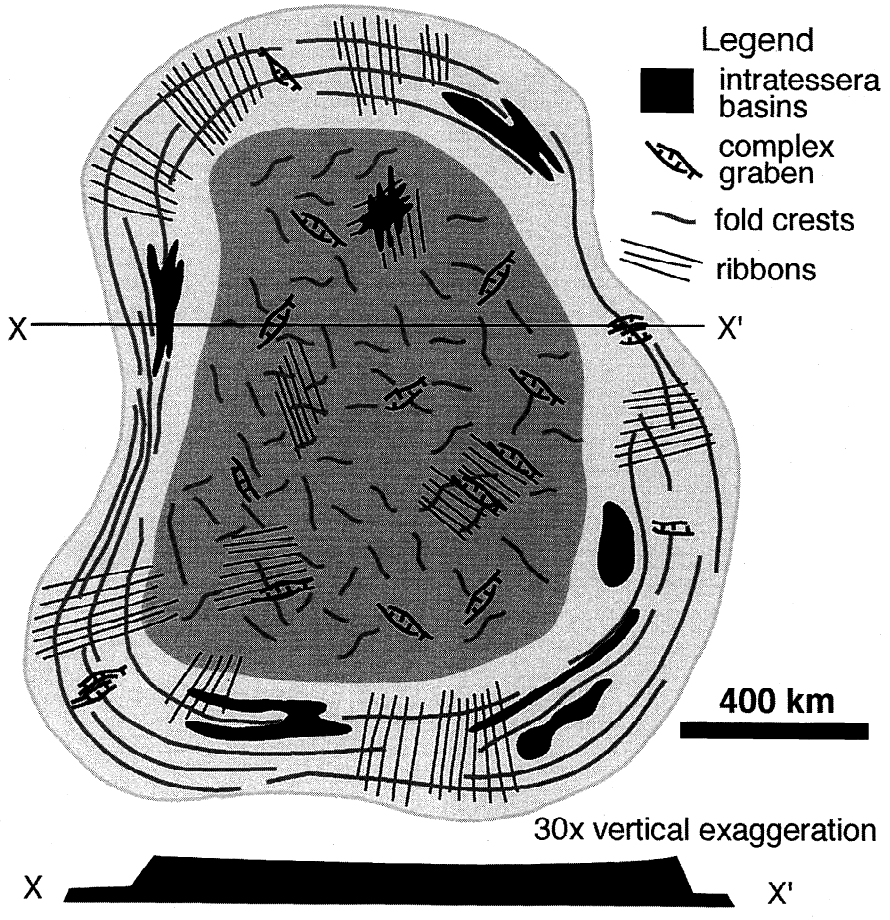

Figure 2. Schematic structure map and topographic cross-section of a typical crustal plateau showing marginal-fold domain (light shading) and interior basin and dome domain (dark shading), ITBs (black), and general patterns defined by tectonic elements (modified from *Hansen et al.* [1999]).

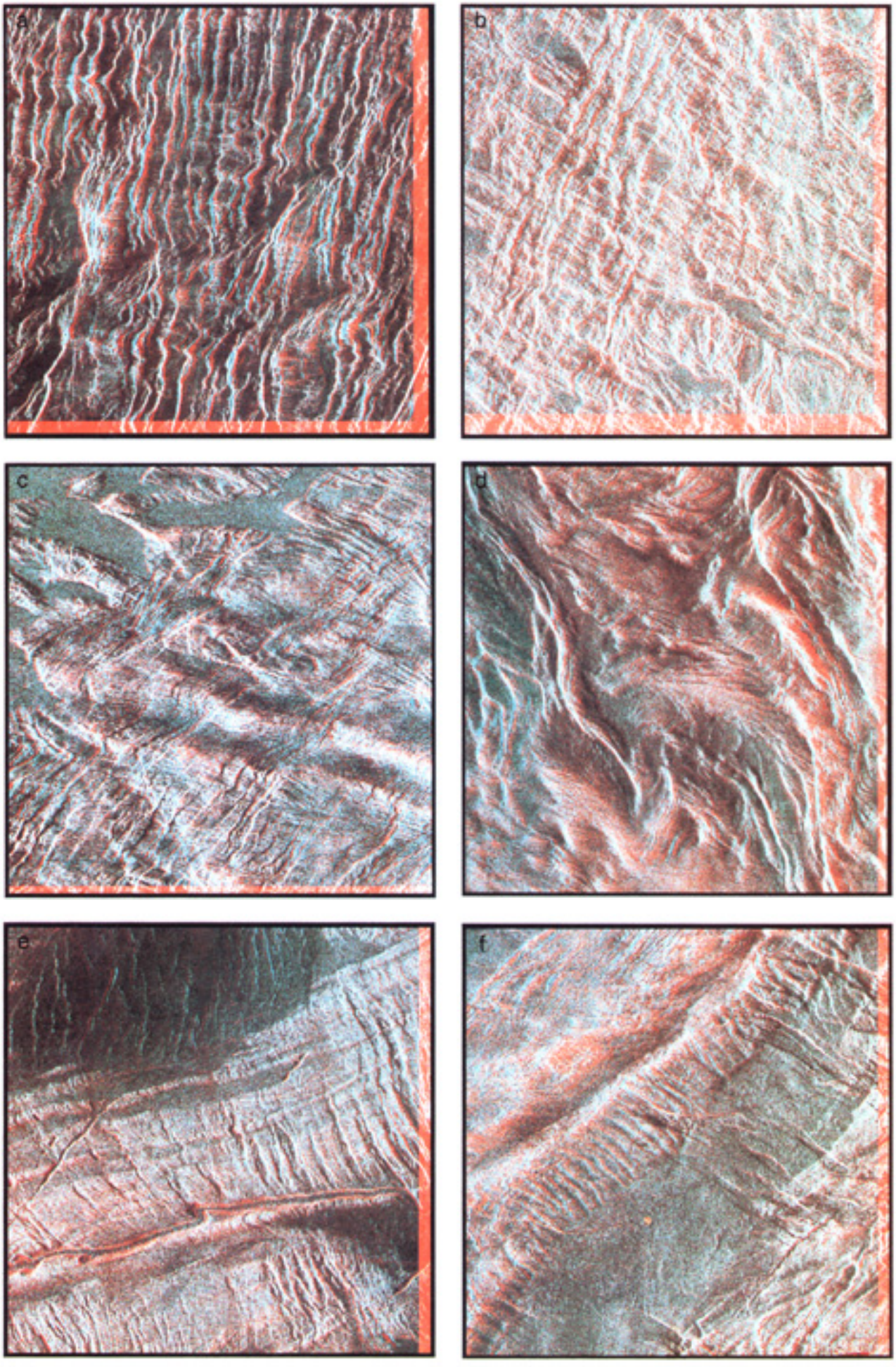
a
b
c
d
e
f

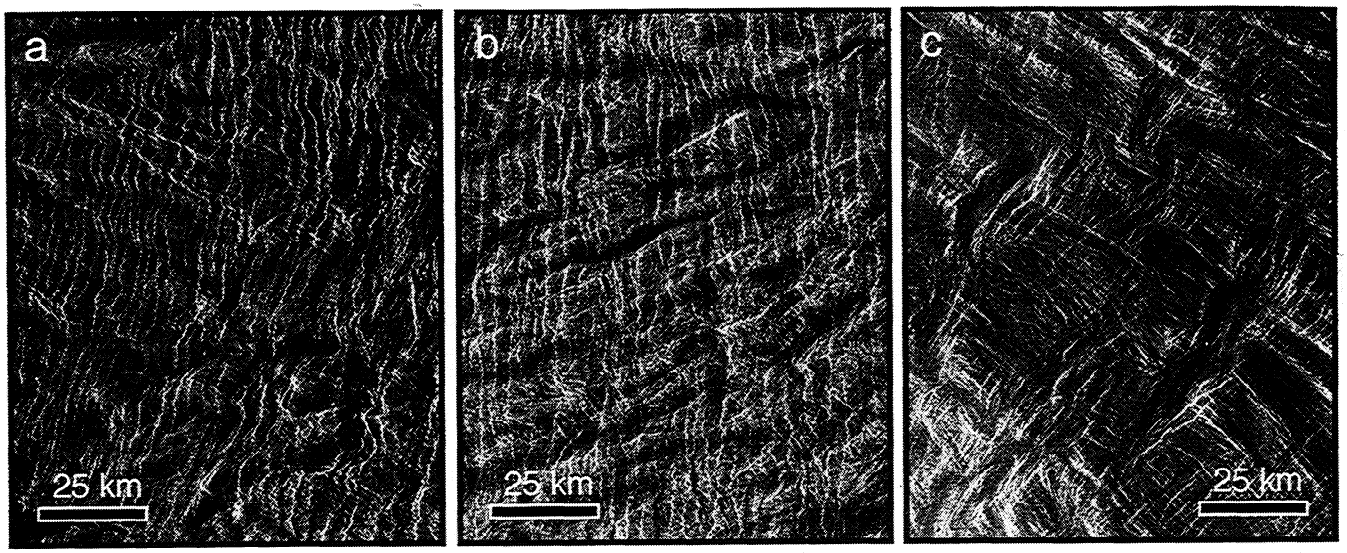

Figure 3. Left look SAR images of 100 x 125 km regions illustrating (a) tensile fracture ribbons from the type location at Fortuna Tessera; image center 58.4°N/13.1°E (from type location); (b) shear fracture ribbons from Thetis Regio; image center 6.8°S/131.4°E, and (c) NE trending late complex graben cutting the crests of NW trending folds; NE trending ribbons are morphologically different than wider, lens-shaped, complex graben [also see *Phillips and Hansen,* 1998, Figure 2]; image, centered at 4.5°N/98.3°E, is from northeast Ovda Regio.

2. Structural and Kinematic Analysis

Each crustal plateau except Phoebe hosts intratessera basins (ITBs) filled by lava flows [*Banks and Hansen*, 1998; 1999] and at least three distinct tectonic elements: ribbons (extensional troughs), folds, and complex graben [*Hansen and Willis*, 1996, 1998; *Hansen et al.,* 1997]. Ribbons occur across crustal plateaus, and fold-graben relations define two structural domains: (1) marginal fold terrain, and (2) interior basin and dome terrain dominated by either folds or graben (Figures 1 and 2) [*Hansen et al.,* 1997; *Ghent and Hansen,* 1999]. Eastern Ovda also hosts a unique tessera fabric that exhibits ribbons and folds but no graben, originally termed "lava flow terrain" due to its resemblance to the surface of a pahoehoe lava flow (Plate 1c; *Hansen and Willis* [1996]; later called "domain I" by *Ghent and Hansen* [1999]. *Hansen and Willis* [1998] illustrated that ribbons are represented by two end-member types: tensile fracture ribbons and shear fracture ribbons [Figures 3 and 4 and Plates 1a and 1b]. These distinctions are based on structural and kinematic analysis, which seeks to understand the mechanical relations between structural elements preserved on planetary surfaces that reflect surface strain resulting from stress within the crust or lithosphere. Structural and kinematic analysis follows a specific methodology [e.g., *Ramsay and Huber*, 1983, 1987; *Twiss and Moores*, 1992; *Davis and Reynolds*, 1996; *Price and Cosgrove*, 1990; *van der Pluijm and Marshak*, 1997], and any kinematic criticism must also follow this methodology. Kinematic analysis involves several, typically iterative, tasks: (1) identify and differentiate different structural elements or suites of elements; (2) determine geometry, orientation, and spatial distribution of each structural suite; (3) determine temporal relations between and among structural suites, recognizing that they could have formed synchronously, each could also be partially or wholly reactivated, and determination of temporal relations requires knowledge of deformation mechanisms; and (4) develop a coherent kinematic and mechanical model that addresses each

Plate 1. Three-dimensional (3-D) stereo images constructed from cycle 1 (red) and 3 (blue-green) FMIDR (full resolution) synthetic aperture radar (SAR) data [*Plaut*, 1993] (each area is ~75 x 75 km with north at the top; view images through red (left eye) and blue glasses for 3-D effect). Locations and regional context of Plate 1c-1e shown in Figure 6. (a) North trending dominantly tensile fracture ribbons (western Ovda Regio; FMIDR 05N065ff40); note that west trending fine lineaments are rare (this could be due to radar angle, or it could be that fine lineaments are rare in this region); (b) NE trending dominantly shear fracture ribbons and WNW trending fine lineaments with local radar-dark flood lava (?) in topographic lows (western Ovda Regio; FMIDR 10S059ff37,38); (c) region enclosing Figure 8 of *Gilmore et al.* [1998] (FMIDR 05S076ff14), see Figure 9 for geologic map interpretation; (d) ultrathin ribbons folded around chevron-like folds (central eastern Ovda Regio "lava flow terrain" [*Hansen and Willis*, 1996]; domain I [*Ghent and Hansen,* 1999]; FMIDR 05S087ff21); the fabric resembles that of a piece of folded corduroy cloth with the cords analogous to the ribbons (note ribbon troughs near limit of SAR resolution bent around the crest of the chevron fold in the south (bottom) central region of the stereo image); (e) intimate temporal relations between short-wavelength fold formation and flood lava flows (frameIet 20 of FMIDR 00N082); and (f) reactivation of early formed ribbons (FMIDR 00N082ff55). See text for further discussion of each image.

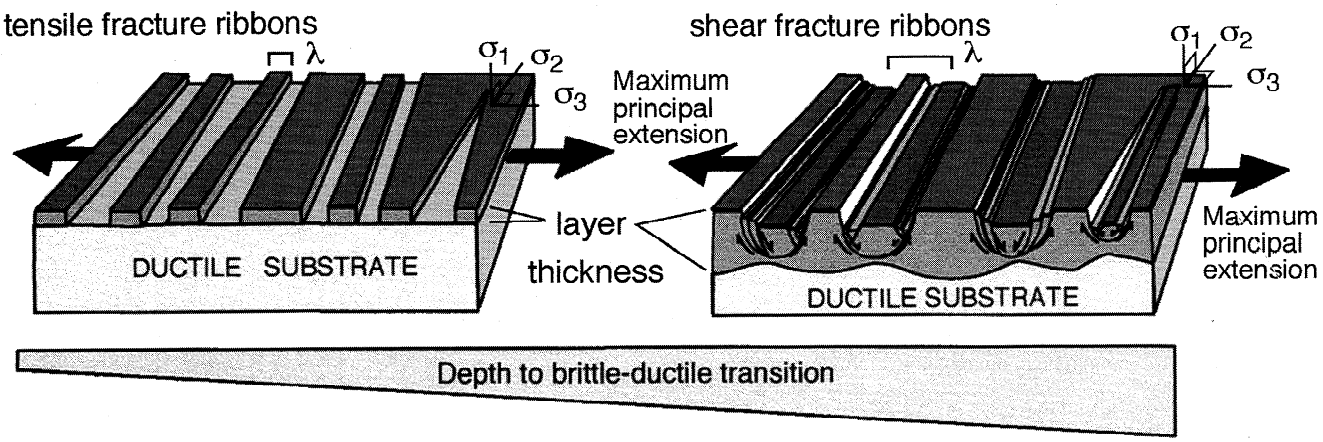

Figure 4. Tensile and shear fracture kinematic ribbon block models [after *Hansen and Willis*, 1998, Figure 8]; dominant wavelength, λ; σ_1, σ_2, and σ_3 are maximum, intermediate, and minimum principal compressive stresses, respectively. Ribbon trough formation, whether by opening of tensile fractures or by trough formation by normal faults, requires a ductile substrate at relatively shallow depth. Opening of tensile fractures would be favored with a sharp brittle ductile transition (BDT) at shallow depth, whereas a deeper BDT would favor shear fracture ribbon structures.

set of constraints. *Gilmore et al.* 's [1998] criticism of *Hansen and Willis* [1996, 1998] violated steps 1, 2, and 3, and therefore, also 4.

2.1 Step 1: Structural Element Identification

2.1.1. Ribbons and graben. The different morphologic characters of ribbons and graben and of tensile fracture and shear fracture ribbon fabrics are visible in high-resolution Magellan left-look synthetic aperture radar (SAR) images (Figure 3) and Magellan three-dimensional stereo imagery (Plates 1a, 1b, and 1c; see *Hansen and Willis* [1998] for a complete discussion). Ribbons (Figures 3a and 3b and Plates 1a and 1b) are defined as regularly spaced, alternating narrow ridges and troughs with large length-to-width aspect ratios. Graben (Figure 3c and Plate 1c) are wider and shorter than ribbons, exhibit many more internal lineaments, and do not show a regular spacing [*Hansen and Willis*, 1996, 1998; *Pritchard et al.*, 1997; *Ghent and Hansen*, 1999]. Ribbons and graben were distinguished in initial analyses of Magellan SAR data; *Bindschadler et al.* [1992a] morphologically differentiated wide "graben" from narrow "steep troughs" (ribbon troughs), in the region illustrated in Figure 3c. They noted that graben widen across fold crests and therefore postdate folds. *Head* [1995] distinguished "wide troughs" or "complex graben" from "narrow troughs" (<~2 km wide, spaced 3-5 km apart, i.e., ribbons) and asserted that narrow troughs may have formed contemporaneously with folds and that wide complex graben formed after both folds and narrow troughs. *Bindschadler et al.* [1992a] did not independently address ribbon and graben temporal relations; they inferred that because ribbons and graben are parallel and both record extension, ribbons and graben both postdate folds. However, the morphologic differences between ribbons and graben suggest that ribbons and graben should be treated as separate structural elements. For example, ribbon troughs do not consistently widen across fold crests like graben. Thus ribbon troughs either have much steeper walls than the graben (and therefore different geometry, as originally recognized by *Bindschadler et al.* [1992a]), or ribbons must have different temporal relations with respect to the folds, or both.

Hansen and Willis [1996] recognized that the previously described steep/narrow troughs ("ribbons") form part of a coherent tectonic fabric comprised of alternating linear ridges and troughs with large length:width aspect ratios; they termed these structures "ribbons." They outlined specific criteria to differentiate ribbons from complex graben; they also presented a preliminary kinematic (and thus temporal) analysis of ribbons, folds and graben. *Pritchard et al.* [1997] presented additional criteria that differentiate ribbons from graben in southwest Fortuna Tessera.

Gilmore et al. [1998] did not differentiate ribbon structures from complex graben, reverting to *Bindschadler et al.*'s [1992a] assumption that they are the same structure. This omission precludes examination of temporal constraints between ribbons and graben and leads to fundamental flaws in their geometric and temporal interpretations of tessera extensional structures.

2.1.2. Tensile fracture and shear fracture ribbons. *Hansen and Willis* [1998] presented a detailed structural and kinematic analysis of ribbon structures, aimed at defining the geometry, kinematic evolution, and tectonic implications of this distinctive structural fabric. Their analysis indicates that ribbon structures exhibit two end-members: tensile fracture ribbons and shear fracture ribbons (Figures 3a, 3b and 4; see also *Hansen and Willis* [1998, Figure 8]). Both ribbon types comprise a fabric of regularly spaced alternating ridges and troughs with large length:width ratios, both are extensional fabrics, and both reflect a rheological structure with a thin brittle surface layer above a ductile substrate. Tensile fracture ribbon troughs result from the opening of tensile fractures (mode I) within the thin surface layer, whereas shear fracture (mode II) ribbon troughs result from deformation and displacement of this layer along trough-bounding dominantly "shear fractures" or normal faults. The terms tensile fracture and shear fracture are used to describe the manner in which the brittle layer fails as defined by Griffith-Coulomb failure analysis [*Hansen and Willis*,

1998, Figure 12]. *Hansen and Willis* [1998] introduced the term "shear fracture ribbon" specifically to avoid confusion with complex graben, whose troughs are also bounded by normal faults. Although tensile fracture and shear fracture ribbons are broadly morphologically similar (Figures 3a, and 3b and Plates 1a and 1b), the differences between them provide clues to the dominant deformation mechanism responsible for end-member ribbon formation. Tensile fracture ribbons show distinct paired alternating bright and dark lineaments, matched trough walls that would display a close fit if closed, V terminations of opposite trough walls, and relatively few internal lineaments. Shear fracture ribbons display many interior lineaments that contribute to a less distinct alternating ridge and trough morphology, trough walls that cannot be closed, and opposite trough walls that show broadly parallel terminations, indicating that trough floors ramp up to meet ridge tops [*Hansen and Willis*, 1998, p. 337]. Examples of both types of ribbons exist; tensile fracture ribbons dominate at southwestern Fortuna Tessera, whereas shear fracture ribbons dominate at eastern Ovda and Thetis [*Hansen and Willis*, 1998]. The specific method used to estimate extension depends on ribbon type, as does determination of structural wavelength, with implications for layer thickness [*Hansen and Willis*, 1998; *Ghent and Hansen*, 1999].

Gilmore et al. [1998, p. 16,814] acknowledged the existence of geometric and kinematic differences between tensile fracture ribbons and shear fracture ribbons, but decided "for clarity" to disregard *Hansen and Willis*' [1998] treatment of shear fracture ribbons. *Gilmore et al.* [1998] then attempted to illustrate that not all ribbons are bounded by tensile fractures and that some are bounded by normal faults, or shear fractures, to use the term introduced by *Hansen and Willis* [1998]. Thus they stated their intent not to treat shear fracture ribbons, yet subsequently reinvented the concept for such structures. For example, ribbons from Thetis illustrated in *Gilmore et al.* 's [1998] figure 10 are shear fracture ribbons, not tensile fracture ribbons as *Gilmore et al.* [1998] imply; thus it is not surprising that these ribbons do not show tensile fracture ribbon morphology. Furthermore, *Gilmore et al.* [1998] cited *Pritchard et al.* [1997] as proposing that ribbons in Ovda Regio are tensile fracture ribbons with specific estimates of extension. However, *Pritchard et al.* [1997] mapped tensile fracture ribbons in southwestern Fortuna Tessera; *Ghent and Hansen*, [1999] demonstrated that shear fracture ribbons dominate across eastern Ovda and provided extension estimates. Because not all ribbons are tensile fracture ribbons, *Gilmore et al.*'s [1998] critique of these previous works is not relevant.

2.2. Step 2: Geometry of Structural Elements

Crustal plateau tessera fabric includes ribbons, folds, and complex graben; the geometry of each must be independently determined.

2.2.1. Ribbons. *Hansen and Willis* [1996, 1998] described tensile fracture ribbons as composed of parallel bright and dark lineaments. They used the term "parallel" in the loose sense to mean that if one wall bends to the west, so does the opposite wall (Figure 5). *Gilmore et al.* [1998] argued that changes in width along the length of individual ribbon troughs in southwest Fortuna Tessera (their Figures 2b, 2c, and 3) illustrate that these ribbons could not have a tensile fracture origin. However, as figure 5 illustrates, the width across a tensile fracture must change along its length, from zero at the ends to some finite width in the middle. Obviously, troughs with V terminations cannot have walls that are parallel along their entire lengths. A block diagram illustrating surface constraints on ribbon geometry shows walls that are parallel in the sense outlined above [*Hansen and Willis*, 1998, Figure 7]. In contrast, shear fracture ribbons do not require a change in width along trough length (Figure 5b). Canyonlands graben provide an excellent analog; relatively regularly spaced graben bounded by very steep normal faults (that reactivate joints) show little change in width along trend [*McGill and Stromquist*, 1979, Figure 6]. Thus *Gilmore et al.'s* [1998] data favor a tensile fracture mechanism over a shear fracture mechanism for Fortuna Tessera ribbons, in agreement with previous analyses [*Hansen and Willis*, 1996, 1998; *Pritchard et al.*, 1997].

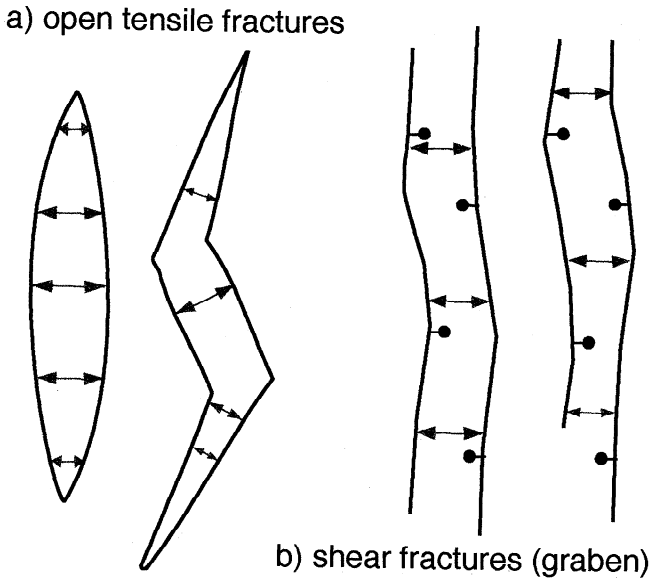

Figure 5. Plan views of (a) tensile fractures, and (b) shear fractures (graben).

Gilmore et al. [1998] (abstract, p. 16,813) stated that "a major question centers on the interpretation of specific lineaments within tessera as graben (bounded by faults dipping ~60°) or, alternatively, open tensile fractures (dipping ~90°)." *Gilmore et al.* [1998] used "graben" for any normal-fault-bounded trough; and they did not differentiate between morphologically different ribbons and complex graben. Block diagrams of ribbon structures (Figure 4) show a wide range in the dip of ribbon-bounding structures [see also *Hansen and Willis*, 1998, Figure 8]. Thus the dip of ribbon-bounding structures is not a particularly critical factor to differentiate ribbons from other structural elements, although it is important to consider in determining the end-member ribbon type. *Gilmore et al.* [1998, p. 16,828] incorrectly stated that *Hansen and Willis* [1996, 1998] "...assume[d] that [ribbons] predated the folds and then measure[d] the 'embayment angle' β." However, *Hansen and Willis* [1998] used embayment relations and dip projection relations [*Mankin*, 1950] only to describe the tops and bottoms of ribbon ridges and troughs, respectively, not to constrain dip. *Hansen and Willis* [1996, p. 302] did not assume any temporal relation; they explored two different scenarios, stating "...the

relation of β to three-dimensional ribbon geometry depends upon whether ribbons postdate or predate folds," and then they discussed the implications of embayment relations for each scenario. In addition, two other lines of evidence, independent of ribbon-fold temporal relations, suggest that trough-bounding structures at southwest Fortuna Tessera have steep dips [*Hansen and Willis*, 1998, pp. 325-332, Figures 3-6 and Table 1]: (1) detailed radargrammetric analysis suggests that ribbon trough-bounding structures are steep; and (2) the narrow width of the dark shadowed and bright laid over regions that define ribbon trough walls imply steep wall dips. The approach outlined by *Gilmore et al.* [1998] is similar to the method presented with mathematical proofs by *Hansen and Willis* [1998] and offers no new geometrical constraints.

Gilmore et al. [1998, pp. 16,828-16,830] attempted to constrain trough wall dip using other geometric considerations. We feel that their efforts are overly simplified. Many workers have noted that if a graben cuts preexisting folds, graben width will increase with fold height, and therefore graben will widen across fold crests [e.g., *Baldwin*, 1971; *McGill*, 1971; *Golombek*, 1979]. As *Gilmore et al.* [1998] noted, at least 130 m of elevation change is required to resolve a change in graben width in full resolution Magellan images, assuming 60° dip of graben-bounding normal faults. Uncertainties of feature edges due to data resampling may also affect width estimates [e.g., *Saunders et al.*, 1992; *Gilmore et al.*, 1998]. Thus it is not fruitful to use trough wall deflections to constrain dip across low-relief topographic features. Recognizing this, *Hansen and Willis* [1998] used trough wall deflections at high-relief features (height change of >1 km), where trough widening, if present, would be maximized. Only local measurements were made to avoid width changes along the entire trough length, which are likely to occur regardless of trough origin [*Hansen and Willis*, 1998, Figures 2 and 11]. *Hansen and Willis* [1998] analyzed three areas with topographic relief from 1.08 to 1.94 km; trough walls with 60° dips should exhibit corresponding width increases of 1.25-2.24 km. Such widening is not observed for ribbon troughs, and minimum trough wall dips of 84° are consistent with observed trough deflections across fold crests at the areas examined.

2.2.2. Ribbon and fold wavelength. As stated by *Hansen and Willis* [1998], the critical characteristic of ribbon fabric is not the dip of trough-bounding structures but rather the regular spacing of ribbon ridges and troughs, which reflect a structural wavelength and imply a very shallow depth to the brittle-ductile transition (BDT). Ribbon ridge-trough spacing deduced from *Gilmore et al.'s* [1998, Figures 5-8] geologic maps are consistent with ribbon ridge-trough spacing documented in previous studies that covered larger regions of their respective map areas [*Hansen and Willis*, 1996, 1998; *Pritchard et al.*, 1997; *Ghent and Hansen*, 1999]. Thus *Gilmore et al.* [1998] actually agree with the critical aspects of ribbon geometry documented in previous studies.

Ribbons and folds are commonly spatially correlative in crustal plateaus. Long-wavelength folds (15-30 km) include long (hundreds of kilometers), upright, gentle cylindrical folds with axes generally parallel to and coincident with plateau margins; and short (~50 km), upright, gentle folds with varying orientation, preserved within plateau interiors (Figures 2 and 6) [*Ghent and Hansen*, 1999]. Fold wavelengths and amplitudes stated by *Gilmore et al.* [1998] are similar to those noted by others [e.g., *Bindschadler et al.* 1992a; *Hansen and Willis*, 1996, 1998; *Ghent and Hansen*, 1999]. Because wavelength is a function of shortening and depth to BDT, *Gilmore et al.*'s [1998] wavelength estimates correspond to estimates of minor shortening and depth to BDT during fold formation of ~ 6 km, in agreement with previous work [*Brown and Grimm*, 1997; *Ghent and Hansen*, 1999].

2.3. Steps 3 and 4: Temporal Relations and Kinematic Models

Rigorous geometric analysis is necessary but not sufficient for robust kinematic analysis. An example from *Gilmore et al.* [1998] serves as an illustration. *Gilmore et al.* [1998, Figures 2d and 4] argue that the shifting of ridge crests away from incident radar illumination along ribbon troughs relative to ribbon ridges provides evidence that folds predate ribbons. However, these relations constrain only surface geometry, that is, that fold crests within the ribbon troughs lie topographically below fold crests along the ribbon ridges. *Hansen and Willis* [1998, Figure 6] discussed this very geometry for spatially associated fold and ribbon structures; block diagrams [*Hansen and Willis*, 1998, Figure 9] show how the same geometry could be achieved through opposite temporal relations (ribbons predating folds and ribbons postdating folds). Both scenarios result in the same surface geometry and thus would appear precisely the same in radar imagery. As discussed by *Hansen and Willis* [1998], surface geometry cannot impose relative temporal constraints on ribbon and fold kinematics.

Gilmore et al. [1998, Figure 2d] also attempted to illustrate that Fortuna ribbon troughs (thin ribbons of *Pritchard et al.* [1997]) widen across fold crests and therefore postdate fold formation. *Gilmore et al.* [1998] emphasized that in this area extensional structures trend subparallel to the radar look direction and therefore show clearer morphology. However, their Figure 2d illustrates that (1) thin ribbon troughs trend ~45° to the radar, not subparallel and (2) there is no consistent correlation between ribbon trough width and fold crests. Some ribbon troughs are slightly wider across fold crests and others are clearly narrower along fold crests and wider in fold valleys due to the natural variation in trough width. Thus, if ribbon troughs are bounded by ~60° dipping walls (as asserted by *Gilmore et al.* [1998]), this relation argues that ribbons predate folds (i.e., if trough-bounding faults dip 60° and if troughs formed after the folds, then troughs should preferentially and consistently widen across the fold crests; they do not); if ribbon troughs are bounded by steep walls (>75°), temporal relations with respect to folds are unconstrained by these relations [*Hansen and Willis*, 1998, Figures 3 and 6, pp. 324-332].

These same arguments illustrate the difficulty of using fine lineaments to determine temporal relations [see *Gilmore et al.*, 1998, Figure 4]. The origin(s) of such fine lineaments (there may be more than one type—each with a different origin; an example of one type is illustrated in Plate 1b) is indeed a mystery to us, although we can safely state that they are likely not lineaments related to stretching of a ductile substrate as proposed by *Hansen and Willis* [1996]. Until a mechanism of formation (including identification as either primary or secondary structures) can be robustly determined, there are no constraints on whether fine lineations formed before, during or after extension related to ribbon formation.

Using the present data one cannot uniquely determine if the fine lineaments are primary or secondary structures or if the fine lineaments are similar. Some fine lineaments look like brush strokes; these could represent primary structures form

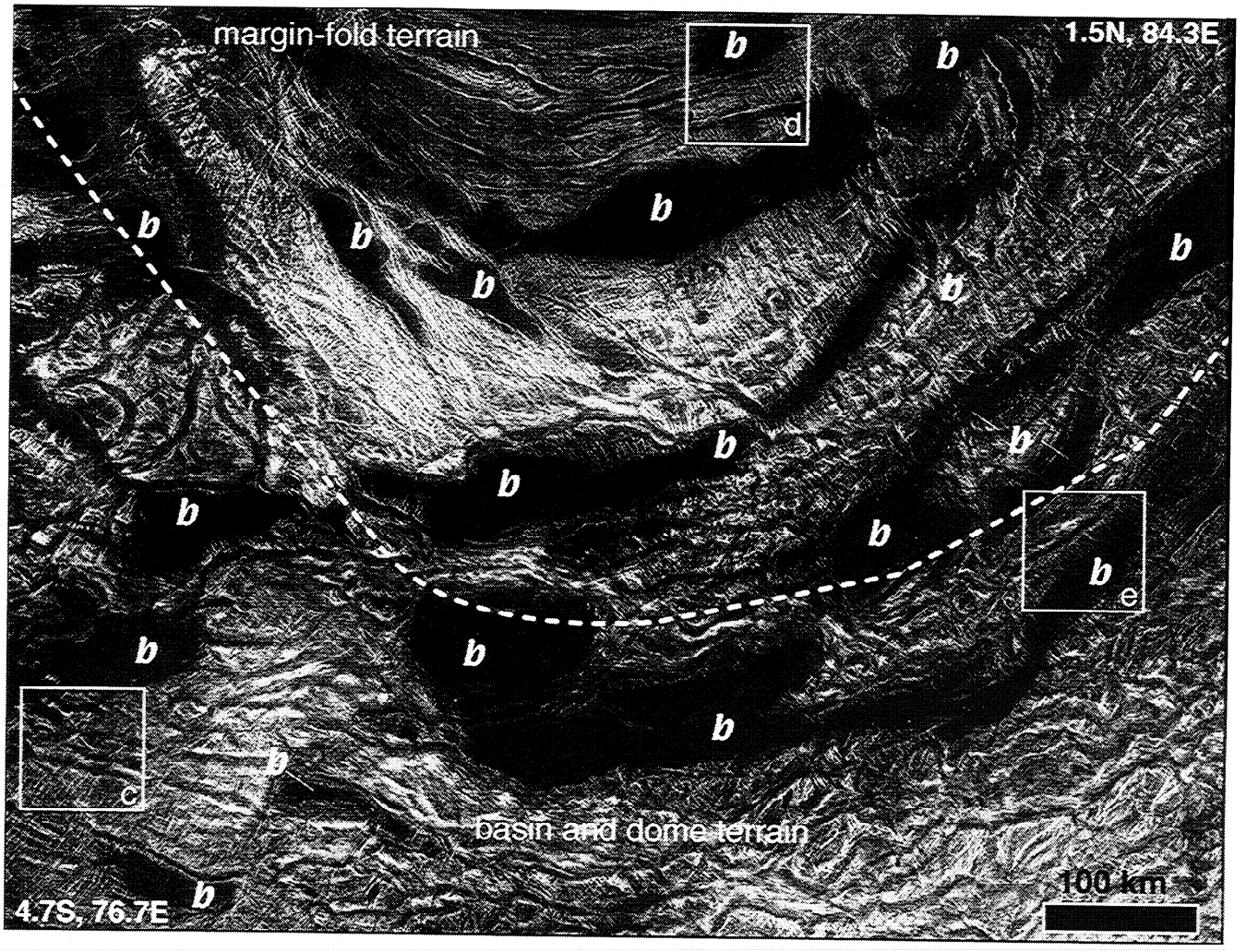

Figure 6. SAR image of north central Ovda Regio showing marginal fold and basin and dome domains, ITBs (***b***), and local and regional context of 3-D images shown in Plates 1c, 1e and 1f. Dashed line marks the broad transition between the marginal fold domain and the basin and dome domain. Note that ribbon trends continue uninterrupted between domains.

by accumulation of fine wind-blown particles. Another family of fine lineaments that parallel fold crests could represent parasitic folds, which form with parallel trends to their hosts by deformation of thinner mechanical layers [*Ramsay and Huber*, 1987; *Twiss and Moores*, 1992], and as such, they could form at the same time as the "host" long-wavelength folds [*Ghent and Hansen,* 1999], or they could form before the long-wavelength fold and serve as mechanical anisotropy that affects later long-wavelength fold formation [e.g., *Watkinson*, 1976, 1983]. Layering of crustal plateau material is not unexpected, as discussed below.

In addition, fine lineaments associated with tensile fracture ribbons may be quite different in mechanism and relative timing than fine lineaments associated with shear fracture ribbons. Formation of tensile fracture ribbons results in a newly exposed surface in the ribbon trough, whereas shear fracture ribbon troughs preserve the original surface (Figure 4). In three-dimensional (3-D) stereo images, some tensile fracture ribbons (Plate 1a) lack fine lineaments, whereas some shear fracture ribbons (Plate 1b) show abundant fine lineaments. Because the fine lineaments are below the resolution of Magellan SAR imagery, strong arguments for their formational mechanism(s), or even identification as primary or secondary structures, are extremely difficult to justify.

2.3.1. Rheology and competent layer thickness. To go from a geometric model to a unique kinematic understanding of structures requires more information. What are the limits and character of structural elements at depth? What deformation mechanisms were involved in their formation? We need some way to constrain deformation mechanisms and/or to look beneath the surface to begin to understand the kinematic evolution of ribbons and folds.

Understanding deformation mechanisms (and subsurface structure) requires knowledge of material rheology and rheological structure during deformation. Clues about rheological structure can be gained from regular structural spacing or wavelength, as recognized by *Ramberg* [1955]. Layer instability theory illustrates that dominant wavelength:thickness ratios (l:d) exist for both contractional and extensional structures. The nature of the deformation, or layer instability (e.g., whether contractional or extensional, brittle or ductile, tensile or shear fracture brittle failure),

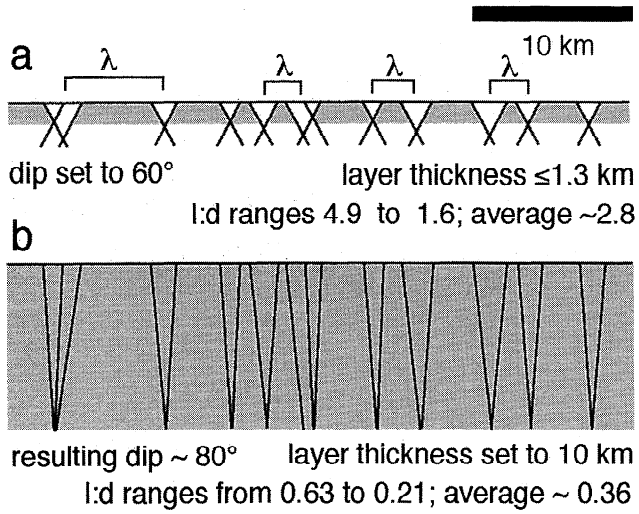

Figure 7. East-west cross-sections constructed through the central part of *Gilmore et al.'s* [1998] Figure 7 illustrating ridge (shaded) and trough (white) spacing. Wavelengths (graben trough center to graben trough center) range from 6.4 to 2.1 km with an average value of 3.63 km. (a) Cross-section employing a 60° dip for trough-bounding structures as suggested by *Gilmore et al.* [1998], resulting in a maximum layer thickness estimate of ~1.3 km, and l:d ranging from 4.9 to 1.6, with an average value of 2.8. (b) Same cross section using a 10-km layer thickness suggested by *Gilmore et al.* [1998]; in this case, trough-bounding structures dip ~80°, and l:d ranges from 0.6 to 0.2 with an average value of 0.36. These cross sections illustrate that a 60° dip and a 10 km layer thickness are mutually exclusive. See *Gilmore et al.* [1998, Figure 1].

affects specific l:d ratios. First-order questions, with respect to ribbon and fold kinematics, are, in descending order of importance: (1) What are their dominant wavelengths? (2) Are structures extensional or contractional? (3) Are they dominantly brittle or ductile? With respect to ribbon end-member type, second-order questions can also be addressed. At what scale is deformation brittle or ductile (pinch and swell)? If brittle, did failure occur along tensile fractures or shear fractures [see *Lloyd et al.*, 1982, *Price and Cosgrove*, 1990]? For a given rheological profile, answers to these questions result in more specific l:d ratios [*Hansen and Willis*, 1998].

2.3.1.1. Ribbons: Ribbon spacing reflects competent layer thickness during ribbon formation. Competent layer thickness and depth to BDT during ribbon formation is much better constrained than the 0.5-10 km range asserted by *Gilmore et al.* [1998]. A centrally located cross section of *Gilmore et al.'s* [1998] Figure 7 displays an average wavelength across nine ridges of 3.6 km (Figure 7a; in agreement with shear fracture ribbon spacing of 3.5-4.5 km [*Hansen and Willis*, 1998]). Using this spacing and an assumed dip of 60° [*Gilmore et al.*, 1998] for trough-bounding faults yields competent layer thickness ≤1.3 km and an average l:d of 2.8, within the limits for brittle extension [*Lloyd et al.*, 1982; *Price and Cosgrove*, 1990; *Hudleston and Lan*, 1995]. This is a maximum competent layer thickness (assuming 60° dip) because the cross-section assumes no extension. A 10-km depth to BDT [*Gilmore et al.*, 1998] would require minimum fault dips of >80° and an average l:d 0.36 (Figure 7b), clearly violating wavelength analysis [e.g., *Lloyd et al.*, 1982; *Price and Cosgrove*, 1990; *Hudleston and Lan*, 1995]. Ribbon structures in southwest Fortuna Tessera [*Gilmore et al.*, 1998, Figures 5 and 6] and Ovda Regio [*Gilmore et al.*, 1998, Figures 7 and 8] display similar ribbon ridge (tensile fracture ribbons) and ridge-trough (shear fracture ribbons) widths, respectively, to previous estimates [*Pritchard et al.*, 1997; *Hansen and Willis*, 1998; *Ghent and Hansen*, 1999]; therefore ribbon wavelengths and depths to BDT (<2 km) are in agreement with those of previous studies.

Tensile fracture ribbon versus shear fracture ribbon formation depends on layer thickness and tensile strength, σ_0, [*Hansen and Willis*, 1998, pp. 338-339, Figure 12]. A value of σ_0 of 14 MPa [*Schultz*, 1993] results in tensile fracture ribbon formation for brittle layer thickness <1.2 km. Shear fracture ribbons will likely form if brittle layer thickness exceeds this value (assuming the same σ_0). Contrary to statements by *Gilmore et al.* [1998, p. 16,815], Griffith failure criteria indicate that tensile failure and differential stress are indeed related. Tensile fractures form if effective tensile stress exceeds material tensile strength, and if differential stress is <4 times material tensile strength [*Price and Cosgrove*, 1990, pp. 29-30]. In addition, tensile fractures may evolve into "shear fractures" or normal faults at depth [*Angelier et al.*, 1997]. The depth of tensile fracture formation (<1.2 km) with a σ_0 of 14 MPa is consistent with the radargrammetric estimates of shallow (<1 km) tensile fracture ribbon trough depths [*Hansen and Willis*, 1998], indicating the plausibility of tensile fracture ribbons at southwestern Fortuna Tessera.

2.3.1.2. Folds: As noted above, fold wavelengths and amplitudes stated by *Gilmore et al.* [1998] are similar to those noted by others [e.g., *Bindschadler et al., 1992a*; *Hansen and Willis*, 1996, 1998; *Ghent and Hansen*, 1999]. Because wavelength (and amplitude) is a function of shortening and depth to BDT, *Gilmore et al.*'s [1998] wavelength estimates correspond to estimates of minor shortening (<5%) and depth to BDT during fold formation of ~6 km, in agreement with the work by *Brown and Grimm* [1997] and *Ghent and Hansen* [1999].

2.3.2. Temporal constraints. Having assembled all the available information regarding identification, geometry, and rheology for each of the suites of tectonic structures in question, we can now attempt to understand temporal relations. Timing relations can be determined from mechanical considerations and geologic map relations. Timing of tectonic structures depends on deformation mechanism, and any temporal interpretation must be mechanically justifiable. The question with regard to tessera strain history is not whether folds predate extensional structures or vice versa [Gilmore et al., 1998, p. 16,814; Ivanov and Head, 1999], but rather, what is the complete strain history recorded by crustal plateau tesserae. Crustal plateau tessera fabric is composed of three distinct structural elements: ribbons, folds, and complex graben; therefore a dual-stage strain history cannot be assumed a priori.

2.3.2.1. Complex graben timing: Complex graben clearly postdate folds as evidenced by the widening of complex graben troughs correlated with folds crests [e.g., *Solomon et al.*, 1991; *Bindschadler*, 1992a, b; *Hansen and Willis*, 1996, 1998; *Ivanov and Head*, 1996; *Pritchard et al.*, 1997; *Ghent and Hansen*, 1999]. All workers agree that complex graben postdate folds, but temporal relations between ribbons and folds must be rigorously established.

Because ribbons and graben are distinct structures, one cannot employ fold-graben relations in such arguments. However, *Gilmore et al.* [1998, Figure 9] did just this, attempting to establish ribbon-fold temporal relations using a crater deformed by a complex graben. Gilmore crater in Thetis Regio [*Gilmore et al.*, 1998, Figure 9] is cut by complex graben that are both morphologically more complex, and significantly wider (>9 km wide), than regularly spaced ribbons. The complex graben structure cutting Gilmore crater from the north is actually wider than illustrated by *Gilmore et al.*'s [1998, Figure 9b] geologic map, as can be observed in stereo viewing of the SAR image. Shear fracture ribbons that lie ~100 km west of Gilmore crater (Figure 3b) show dominant ridge width plus trough width of 3.5-4.5 km [*Hansen and Willis*, 1998, Figure 11]. Therefore Gilmore crater does not provide evidence that ribbons formed after craters and late in the recorded structural history of Thetis Regio.

2.3.2.2. Ribbon and fold timing: Mechanical constraints: The spatial correlation of ribbons and folds taken together with mechanical (wavelength) considerations leads to a geohistory of tessera surfaces, as discussed by *Hansen and Willis* [1998, pp. 334-336]. In short, spatial correlation of ribbons and folds (and the depth to BDT during their respective formation (i.e., <1-2 km depth during ribbon evolution and ~6 km depth during fold formation)) is most easily accommodated if ribbons predate folds. These mechanical constraints can be extrapolated across individual crustal plateau regions (rather than just addressing local temporal constraints as in the case of crosscutting relations) in which ribbon and fold wavelengths can be determined.

Additional local temporal relations can also be gleaned from 3-D stereo images of central eastern Ovda Regio (Plate 1d). This region was originally called "lava flow terrain" because of the morphologic similarly of the tectonic fabric with that of the surface of pahoehoe lava [*Hansen and Willis*, 1996]. Three-dimensional stereo viewing of this region allows one to delineate ultrathin ribbon structures that are folded around the axes of distinctive, chevron-like folds (note ribbon troughs near the limit of SAR resolution bend around the crest of the chevron-fold in the south (bottom) central region of the stereo image). Hence, here ultrathin ribbons predated short wavelength chevron-fold formation. Both the extremely fine ribbons and folds indicate deformation of an extremely thin (meters to tens of meters thick) competent layer. Lava flow terrain as a morphologic fabric covers a 500 by 600 km region, an area larger than the state of Wyoming; this extremely thin "corrugated" layer was folded along short wavelength chevron-like folds following ultrathin ribbon formation. Any model for the evolution of crustal plateau tessera must be able to accommodate an extremely shallow depth to BDT across this incredibly large expanse of crust.

2.3.2.3. Ribbon and fold timing: Geologic mapping constraints: *Gilmore et al.* [1998, Figures 5-8] argued that their geologic maps provide evidence that folds predate ribbons. We discuss their interpreted geologic and temporal relations below. *Gilmore et al.'s* [1998] arguments hinge, in part, on a proposed material unit pd (deformed plains). According to them, pd lies completely within fold valleys, and therefore postdates folds, yet ribbons cut pd. If this relation could be firmly demonstrated within a regional framework, it might provide temporal constraints; however, there are several problems with the proposed geologic map relations.

1. *Gilmore et al.* [1998, Figures 5 and 6] showed that pd as mapped locally crosses fold crests, and therefore it is not everywhere confined to fold valleys. A unit that crosses fold crests likely formed prior to, not after, folding.

2. The interpretation of pd as a material unit is also problematic because its limits are based solely on radar brightness, but radar brightness is a function of several variables including slope, roughness, and radar artifacts [*Ford et al.*, 1993]. This requires that one must specifically justify that changes in radar brightness are uniquely related to material units. Although this may be relatively straightforward in the expansive regional plains, characterized by little local topographic relief, changes in radar brightness cannot be assumed to be related only to material unit properties in deformed terrain. If one chooses to use material units to constrain temporal relations between different structural elements, one must unequivocally identify the flow units such that other workers can reproduce them. This generally requires images in both look directions because radar artifacts resulting from local topographic effects (which characterize structurally deformed terrain) must be accounted for.

We examined the regions of *Gilmore et al.'s* [1998] Figures 5-8. In each case we studied an area ~100 km^2 centered around their ~38 km^2 map areas using digital Magellan SAR imagery. For Figures 7 and 8 we examined both cycle 1 and cycle 3 data. We discuss our findings below.

In Figure 5 of *Gilmore et al.* [1998], imaged only in cycle 1, folds trend NNE at a high angle to look direction. We found no unique criteria that would justify distinction between radar dark areas on the backslope of folds and *Gilmore et al.*'s [1998] proposed material unit pd; that is, we could not distinguish pd from slope effects. Furthermore, there is no consistent evidence to interpret the radar darkest regions as a flow unit, particularly upon examination of a larger regional area centered about their map area.

In Figure 6 of *Gilmore et al.* [1998], one prefold unit (tr, ridged terrain) and two postfold material units, (pd, deformed plains, and younger ps, smooth plains) are mapped. We agree that ps is likely a material unit, and that it appears to overlie all other units and therefore it represents the youngest local geologic event. However, we have two major problems with the areas mapped as pd. (1) The limits of ps are more extensive than shown by *Gilmore et al.* [1998]: the north central pd is actually ps; the area mapped pd is clearly connected to ps, as apparent through examination of a larger regional area; similarly, there is no reason to interpret the small area in the central part of the image as pd rather than ps; if this is a material unit, which is not clear, there is no evidence to suggest that it is anything other than ps; the pd unit in the center of *Gilmore et al.'s* [1998] Figure 6 shows a gradational boundary with ps on both its east and west edges; therefore if pd is a material unit, it could simply be a thinner layer of ps, and it need not be a distinct material unit. Furthermore, this patch of "pd" resides on a fold limb facing away from radar, and therefore the apparent absence of fine-scale lineaments that *Gilmore et al.* [1998] apparently used to distinguish tr from pd may be due to slope effects. (2) The large region of pd in the southwest part of *Gilmore et al.*'s [1998] Figure 6 clearly hosts NW to WNW trending lineaments parallel to the lineaments that Gilmore et al. use to characterize tr. Thus there is no basis to interpret this pd as a unique material unit, distinct from tr. Furthermore, unit ps provides no temporal constraints for ribbon-fold formation.

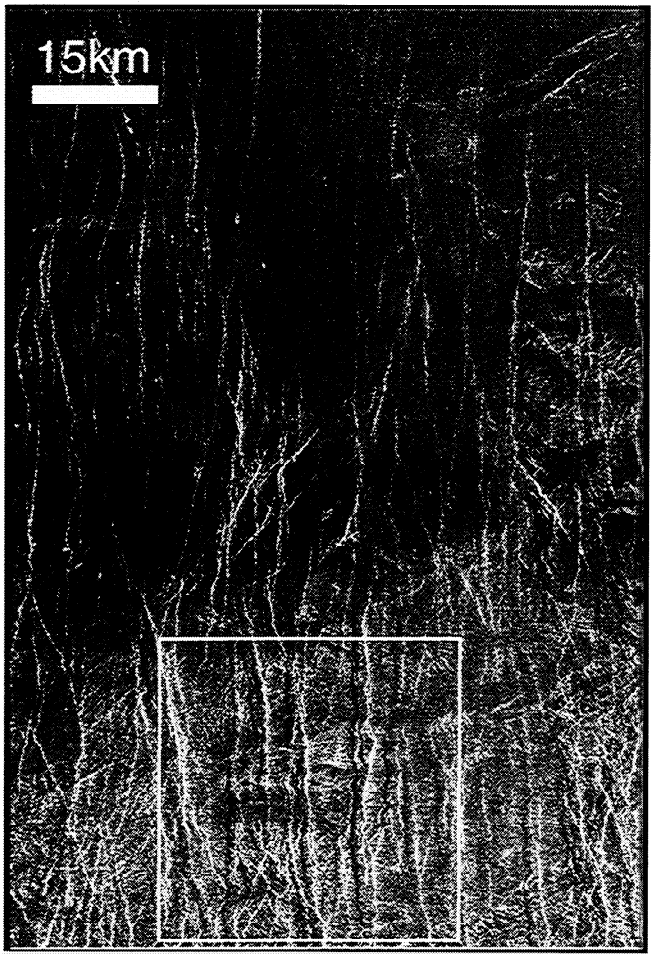

Figure 8. SAR image (80 by 120 km, centered at 6°N/63.4°E) providing regional context for the area of *Gilmore et al.'s* [1998] Figure 7 map area (box). Note that possible east trending "folds" (e.g., dark regions marking "fold valleys" in the center of the box) cannot be traced outside the bounds of the boxed area. In addition, north trending ribbon structures are modified by variable lava flow flooding and structural reactivation. Any temporal constraints that were determined within this region would be difficult to apply with confidence to regional crustal plateau deformation and evolution.

Figure 7 of *Gilmore et al.* [1998] (Figure 8) hosts folds that trend generally parallel to radar look direction, and thus radar artifacts resulting from fold limbs are less likely to be problematic; however, the location of fold crests becomes much less constrained. This region is not an acceptable area to attempt to firmly constrain temporal relations between crustal plateau ribbons and folds for several reasons. (1) The regional area includes several relatively young tectonic features that could affect geologic relations within the map area. (2) The proposed gentle warps in this area are not representative of folds that characterize crustal plateau folds [*Ghent and Hansen,* 1999], and in fact, the regional extent of the folds (warps?) is hard to follow beyond the limits of the *Gilmore et al.* [1998] map area. (3) The ribbons in this region show a different character than type shear fracture ribbons; regional examination illustrates that several episodes of flood lava and structural reactivation events have likely contributed to the preserved surface relations although original ribbon spacing is probably preserved (Figure 8). Therefore any temporal constraints gleaned from cross cutting relations in this region can not be extrapolated with confidence to crustal plateau ribbon-fold timing.

In Figure 8 of *Gilmore et al.* [1998], the area that is encompassed (Figure 6c) shows fold axes subparallel to the radar; thus fold locations are difficult to constrain. We examined cycle 1 and cycle 3 data for the area surrounding and including *Gilmore et al.'s* [1998] Figure 8 (Plate 1c) and constructed a geologic map (Figure 9). Within this region, low-relief alternating topographic ridges and troughs, characteristic of gentle crustal plateau marginal folds trend WNW. Closely spaced (~0.5 km) bright lineaments describe a pervasive fabric parallel to the fold crests; these lineaments appear on both fold limbs (facing toward and away from incident radar), along fold crests, and in fold troughs (Figure 9). NE trending shear fracture ribbons are developed throughout the region with troughs and ridges generally 2-4 km wide and 1-2 km wide, respectively. A single prominent NE trending complex graben (~10 km wide, ~25 km long) in the NW corner of the image shows multiple interior lineaments and clearly truncates three fold crests. The fine lineaments are visible along the ribbon ridges and troughs, and in low portions of the complex graben. Viewed in stereo, they impart a corrugated appearance to the large folds. Flood lava flows occupy the topographically low area NW of the complex graben and forms the southern edge of a prominent ITB (Figure 6). No fine lineaments or other structures deform the flood lava. Flood

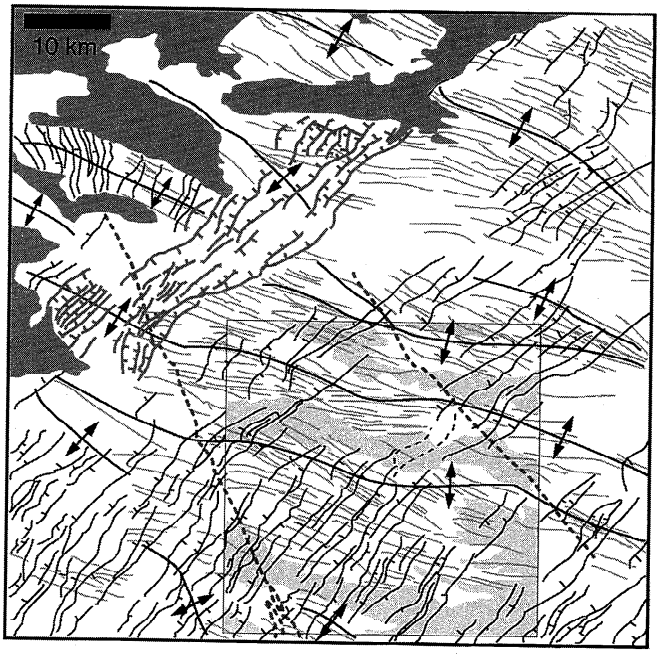

Figure 9. Geologic map of FMIDR 05S076ff14 (Plate 1c) showing NE trending ribbon fabric (solid line with tick on trough side where determinable), WNW trending fold crests, WNW trending fine lineaments (folds?; shaded lines), a single NE trending complex graben structure (gray lines with ticks on trough side), flood lava flow(s) (solid shading), and late NW trending fractures (?; dotted shaded lines). Box shows location of Figure 8 of *Gilmore et al.* [1998]; lightest shading shows the location of their proposed material unit "pd."

lava embays some large fold synforms as well as between some fine lineaments, indicating that the fine-scale lineaments in this region are topographically high, possibly subsidiary folds superimposed on the larger folds, and that flood lava flows postdate formation of both the large folds and the fine lineaments. Two faint NNW trending fractures(?) transect the region and appear to cut all other features.

The flood lava flows appear to both locally embay the complex graben (postdate) and be cut by the graben structures (predate) and thus may be broadly synchronous with complex graben formation. The complex graben also clearly truncates and postdates the large fold crests and likely the fine lineaments. The ribbon fabric trends at a high angle to the fine lineaments and large folds. As discussed above, surface geometry (even that constrained by 3-D stereo data) alone cannot uniquely constrain ribbon-fold temporal relations. Because ribbons and folds both predate late flood lava, robust ribbon-fold timing relations cannot be deduced using crosscutting relations at this location, although mechanical relations, discussed below, may provide temporal clues.

Because the fine-scale lineaments which *Gilmore et al.* [1998] presumably used to differentiate tr from pd are prominently displayed across the entire region, including along all fold crests and valleys and within pd itself (Figure 9 and Plate 1c), there is absolutely no evidence to support the interpretation of pd as a material unit distinct from tr.

Gilmore et al. [1998] also attempted to use craters to constrain fold timing. *Gilmore et al.* [1998, 1997] argued that folding destroyed preexisting impact craters. However, this interpretation cannot be reconciled with the shortening recorded by folds; 5% shortening [*Ghent and Hansen,* 1999] translates into a crater ellipticity of only 1.05. Even 75% shortening would introduce a crater ellipticity of 4, which should be clearly visible given the cylindrical nature of the folds. Highly elliptical craters have not been observed [*Solomon et al.,* 1991; *Gilmore et al.*, 1997]. Destruction of impact craters by folds is thus not viable. Therefore, either crustal plateaus coincidentally preserve regions initially free of preexisting impact craters or a mechanism other than folding removed preexisting impact craters.

In summary, *Gilmore et al.* [1998] argued, based on proposed geologic relations that long-wavelength folds predated ribbons; however, (1) *Gilmore et al.* [1998] did not differentiate ribbons from late graben (late graben-fold relations do not, and cannot, constrain ribbon-fold timing); and (2) the "material units" proposed by *Gilmore et al.* [1998] to flood fold valleys and predate ribbons either predate folds or are simply fold limbs facing away from radar, not material units, and thus provide no temporal constraints. Thus the geologic relations proposed by *Gilmore et al.* [1998] to demonstrate that crustal plateau folds predate ribbons are not valid.

Evidence for crustal plateau volcanism is most apparent in ITBs (Figures 2 and 6) [*Banks and Hansen*, 1998]. Irregularly shaped ITBs characterized by digitate margins resulting from passive flooding of low viscosity lava into topographic lows occur throughout crustal plateaus; quasi-circular to elongate, fault-bounded ITBs occur preferentially in marginal fold domains [*Banks and Hansen*, 1998]. At least some flood lavas commonly postdate basin deformation, as evidenced by the smooth character of basin fill and presence of volcanic edifices. Detailed examination of an ITB perched along the crest of a broad anticline in Tellus indicates that flood lava postdated orthogonal ribbons and minor folds but predated long-wavelength folds [*Banks and Hansen*, 1999; *Hansen et al.,* 1999]. The crest of the host anticline widens around the basin, apparently the result of strain partitioning during folding. Orthogonality of ribbons and minor folds, similarity in ribbon and minor fold wavelengths, and long-wavelength fold-lava temporal constraints are consistent with the following surface evolution: (1) broadly synchronous deformation (minor orthogonal extension and contraction) of a thin (<2 km) competent layer above a ductile substrate; (2) lava flooding; (3) increase in depth to BDT; (4) continued orthogonal extension and contraction; (5) lava flooding; (6) uplift of the broad anticline with continued increase in depth to BDT, and (7) local late lava flooding in broad synclinal valleys.

Evidence for similar tessera surface evolution is preserved in north central Ovda Regio (Plate 1e and Figure 6). At this location, preserved between two ITBs, broad folds trending ENE host parallel shorter-wavelength folds. A NNW trending extensional fabric cuts the fold crests. Flood lava flows with varying radar return locally fill small wavelength synclines, whereas younger (darker and overlapping) flood lava flows fill broad synclinal valleys. Mutual crosscutting relations between extensional structures and older flood lava flows record temporal relations. Early formed short wavelength synforms were apparently uplifted along long-wavelength anticlines after early flooding. Late flood lava flows embayed broad synclinal valleys. This illustrates that low-viscosity lava flow(s) flooded minor fold valleys prior to uplift along

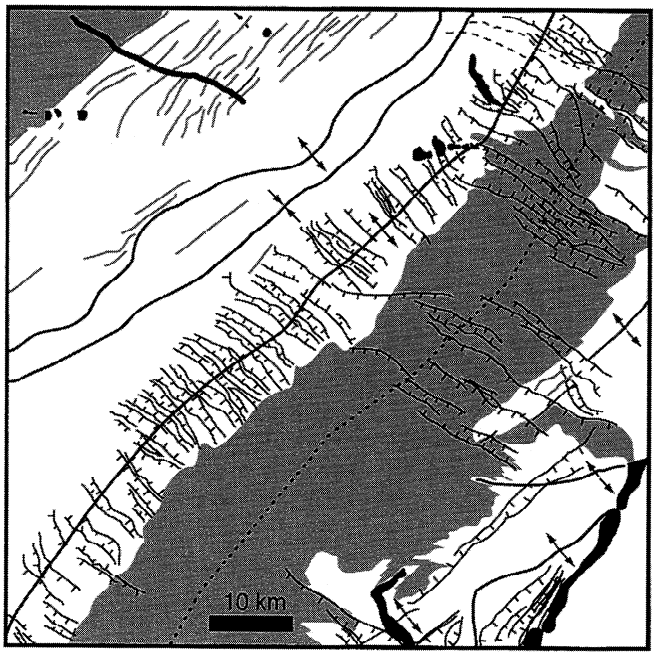

Figure 10. Geologic map of framelet 55 of FMIDR 00N082 (Plate 1f) showing NW trending normal faults (solid lines with ticks on downside) and NE trending fold crests and troughs (thick solid lines; dotted where covered) and fine lineaments (minor folds?; shaded lines), flood lava flow(s) (solid shading), and pit chains (solid). NW trending ribbon structures along fold crests predate flood lava flows in fold valleys; ribbon structures are later locally reactivated after flood lava deposition.

the crests of longer-wavelength folds. Therefore some local lava flows postdated short-wavelength fold formation and predated long wavelength fold formation, whereas late lava flows postdated long-wavelength folding.

In another example from western Ovda, a local flood lava flow postdated ribbon and fold formation and predated complex graben formation; graben formed by reactivation of earlier formed ribbon structures (Plate 1f and Figures 6 and 10). At this location, gentle NE trending warps form broad, flat low-relief topographic ridges. Closely spaced (<1 km) ridges defined by bright lineaments parallel the broad warp crests (Plate 1f). The central band of the large warp lies between two ITBs (Figure 6). A suite of NW trending ribbons occurs along the large warp in the center of the image and ends abruptly at the lava flow boundary; clearly, the lava flow (which follows the synformal valley) postdated formation of these ribbons and the broad fold. A second suite of NW trending extensional structures cuts the flood lava flow. These structures have wider troughs, and their walls are defined by multiple lineaments; we classify them complex graben structures. Numerous pit chains cut all geologic elements. Clearly, the ribbons and folds formed prior to local lava flooding, whereas the wider, complex graben formed after lava flooding. The structures associated with the complex graben most likely reactivated earlier formed ribbon structures, as evidenced by their parallel structural trends. Because of the spatial and temporal overlap of ribbons, folds (short wavelength and long wavelength), complex graben, and flood lava flows and the similarity in trend of ribbon structures and complex graben, one might be able to locally document almost any temporal relations among these geologic elements, but broadly preserved relations indicate that short-wavelength structures (ribbons or folds) predate long-wavelength folds, which dominantly predate complex graben [e.g., *Banks and Hansen*, 1999]. It is equally important to consider that volcanism occurred locally throughout this tectonic evolution.

2.4. Geological History of Crustal Plateaus Surfaces

The geologic, structural, kinematic, and mechanical relations outlined above indicate that in general, extensional strain predates (ribbon fabrics) and postdates (complex graben) contractional strain (long-wavelength folds) across all crustal plateau tesserae examined to date. Furthermore, the tessera surface evolved from a thin (locally extremely thin) competent layer above a ductile substrate to a thicker competent layer with time. This distinctive crustal rheology extended regionally across individual crustal plateaus. As the depth to BDT increased with time, broad gentle folds (defining very little total strain) formed along plateau margins and short variably oriented folds (that also record little total contraction) formed in the interior; local extension formed late complex graben. The fundamentally most important point with regard to understanding surface evolution is that short-wavelength structures predate longer-wavelength structures, indicating an increase in competent layer thickness (and hence depth to BDT) with time across each crustal plateau (except Phoebe). Additionally, flood-type volcanism and tectonism were intimately related throughout tessera evolution.

3. Gravity, Topography, and Tectonism

Tesserae tectonic patterns preserved within individual crustal plateaus correlate with plateau topography and gravity (Figures 1 and 2) [*Ghent and Hansen*, 1999; *Hansen et al.*, 1999]. If tessera terrain formed globally and was later locally uplifted at crustal plateau sites, one would not expect folds to coincide with and parallel plateau margins. Additionally, if deformation postdated plateau uplift, collapse structures should have formed along the plateau margins; yet none have been identified. The correlation of topography-gravity and tessera tectonic patterns strongly favors local over global formation of tesserae.

Plateau topographic profiles also provide further evidence for upwelling. Although mantle downwelling could account for plateau planform shape and size, downwelling results in broad domical topography rather than steep-sided plateau topography [*Bindschadler and Parmentier*, 1990, Figure 13a; *Kidder and Phillips*, 1996, Figure 7]. Plateau topography likely did not result from late collapse because collapse tends to decrease rather than increase slopes, and collapse structures are absent. In contrast, upwelling can accommodate plateau shape, size, and a sharp transition from thick to thin crust. For example, the leading edge of the Hawaiian hot spot marks a sharp transition from thick to thin crust [*Watts and ten Brink*, 1989, Figure 15], and high-resolution bathymetry illustrates the steep-sided character of terrestrial oceanic plateaus [*Smith and Sandwell*, 1997], similar in size to crustal plateaus, and postulated as signatures of deep mantle plumes [*Coffin and Eldholm*, 1994]. Furthermore, given realistic flow laws and thermal budgets, crustal plateau formation by downwelling requires more than 1 b.y. [*Kidder and Phillips*, 1996], whereas mantle plumes can thicken the crust in less than 50 Myr [*Coffin and Eldholm*, 1994; *Farnetani and Richards*, 1994].

4. Crustal Plateaus and Venus Evolution

Although preliminary SAR analysis lent support to crustal thickening as a result of downwelling [*Bindschadler et al.*, 1992a, b], several geologic relations cannot be accommodated by downwelling: (1) an extremely shallow BDT across thousands of square kilometers; (2) early widespread pervasive extension; (3) an increase in depth to BDT with time; (4) minor rather than major shortening associated with broad folds; (5) volcanism associated with all stages of tessera fabric evolution; and (6) the regional topographic profile of crustal plateaus. Furthermore, downwelling would require diapiric sinking and associated crustal transport inward toward individual crustal plateaus, but evidence for such structures is lacking [*Phillips and Hansen*, 1994]. In contrast, relations 1-6 can be accommodated within a magmatic accretion model in which local deep mantle plumes impinge on globally thin lithosphere [*Hansen and Willis*, 1998].

4.1. Post-Magellan Upwelling Model

Gilmore et al. [1998] discussed potential problems with the new upwelling model of crustal plateau evolution and the subsequent geodynamical model [*Hansen and Willis*, 1998; *Phillips and Hansen*, 1998]. However, the flaws *Gilmore et al.* [1998] outlined are not related to problems with either the new upwelling model or the geodynamical model, but rather with *Gilmore et al.'s* [1998] misconceptions of both models. In attempting to criticize the new upwelling model, *Gilmore et al.* [1998] failed to differentiate between fundamentally different pre- and post-Magellan upwelling models. They also misunderstood the role and timing of crustal annealing

processes within the context of the new upwelling model, including crustal annealing processes in general, timing of ribbon formation relative to annealing processes, and implications of annealing for preexisting craters. Finally, within the context of the newly proposed model of Venus evolution [*Phillips and Hansen*, 1998], *Gilmore et al.* [1998] misinterpreted the proposed volcanic mechanism as being responsible for an enhanced global greenhouse, leading to fundamental errors in their criticism.

Gilmore et al. [1998] treated pre- and post-Magellan hotspot models as a single composite model, then attempted to "test" the resulting hybrid model. In discussing a single hotspot model *Gilmore et al.* [1998, p. 16,834] stated, "Ribbon terrain is an essential component in this formulation of the hotspot model for the formation of tessera plateaus, where tesserae are formed by copious amounts of partial melt and magmatic underplating at centers of upwelling [*Phillips et al.*, 1991; *Phillips and Hansen*, 1994, 1998; *Herrick and Phillips*, 1990]." However, contributions by *Herrick and Phillips* [1990] and *Phillips et al.* [1991] predated Magellan and thus recognition of ribbons; ribbon terrain can not be an "essential element" of their models. Furthermore, *Phillips and Hansen* [1994] rejected these pre-Magellan hotspot models based on Magellan data. Pre-Magellan hotspot models [*Herrick and Phillips*, 1990, *Phillips et al.*, 1991] proposed that volcanic rises evolved into crustal plateaus. Magellan data did not support this because crustal plateaus lack large volcanic constructs as are preserved at volcanic rises [*Bindschadler et al.*, 1992a; *Phillips and Hansen*, 1994, 1998; *Bindschadler*, 1995]. Further, these earlier models predicted that crustal plateaus on average should be younger than volcanic rises, contrary to Magellan observations [*Hansen et al.*, 1997; *Phillips and Hansen*, 1998, p. 1493]. Upon recognition of ribbon terrain [*Hansen and Willis*, 1996], a new hotspot model for crustal plateau formation began to emerge [*Hansen et al.* 1997; *Hansen and Willis*, 1998; *Phillips and Hansen*, 1998; *Ghent and Hansen*, 1999].

Gilmore et al.'s [1998] treatment suggests a misunderstanding of the role and timing of crustal annealing processes within the context of the new upwelling model. *Hansen and Willis* [1998, p. 340] stated that ribbon structures require "mechanical annealing of the crust prior to ribbon formation." This statement embraces two important points. First, "mechanical annealing" as used, is a result, not a process; that is, the crust was apparently annealed of preexisting mechanical discontinuities in the form of faults, fractures, and craters. Annealing is a thermally driven process that occurs by the addition of heat, causing the crust to creep. Annealing can occur at many scales, from within an individual crystal to the scale of the entire crust. Annealing in the context of crustal plateau formation would result in the removal of preexisting crustal structures that could otherwise later be reactivated to relieve tectonic stress, muting or preventing the formation of ribbons. The second point is that preserved ribbons formed after crustal annealing. The process of a plume impinging on the lithosphere as modeled by *Gilmore et al.* [1998] could lead to annealing of the crust; indeed, this process could involve magma. Thermal energy could be transferred to the crust through a combination of magmatic intrusion along dikes and/or sills and extrusion (flows) [*Phillips and Hansen*, 1998]. As *Gilmore et al.* [1998] pointed out, the depth at which the crust could undergo creep would be quite shallow, possibly at the surface.

The rheological structure of the crust required for ribbon formation (a thin strong brittle layer above a ductile substrate) could result from the plume-lithosphere interaction; the preserved ribbon structures would form after annealing processes occurred, and after the crust began to cool from the surface downward, thus developing a thin strong brittle layer above a solid-state creeping (ductile) substrate. Undoubtedly in the formation of a crustal plateau there were repeated crustal heating episodes accompanied by extrusive events. As the crust cooled and chilled surface membranes formed, ribbon structures were generated and subsequently buried. The ribbon structures that we see today are those that survived as magmatic output diminished. Furthermore, recent work demonstrates that lava erupted to the surface locally throughout crustal plateau deformation [*Banks and Hansen*, 1999; *Hansen et al.*, 1999] (Figures 6 and 10 and Plates 1e and 1f). Therefore, *Gilmore et al.'s* [1998] assertion that ribbon structures would be accompanied by volcanism appears to be compatible with the hotspot model.

Annealing could be accomplished by some combination of three mechanisms: (1) heat flow from the plume raised temperatures sufficiently to close faults and fractures by solid-state creep, (2) plume partial melting led to widespread surface eruptions, creating a new, relatively deformation-free, upper ~1 km of crust, or (3) partial magmatization of the crust by magmatic injections sealed fractures and faults and annealed the entire crust, promoting solid-state creep throughout. Furthermore, elevated temperature is required to promote a shallow BDT and any of these three processes is potentially capable of achieving this; in fact, we seek mechanisms that would enable both annealing and a shallow BDT.

Gilmore et al. [1998, p. 16,834] further stated "This hotspot scenario predicts that craters which formed on the tessera should record a sequence of extension followed by contraction arising from the gravitational relaxation of the plateau and predicts that (1) craters should display a range of deformation states, including contraction and (2) craters near plateau margins should be preferentially deformed by contraction." However, the new hotspot model does not make these predictions; it predicts that craters that formed prior to ribbon and fold formation were wiped out prior to ribbon formation by the annealing process described above [*Hansen and Willis*, 1998].

We investigated the mechanism of annealing by partial magmatization to evaluate the temporal behavior of a shallow BDT. A cooling half-space model was used; the initial temperature resulted from the mixing of a magma column (using its average temperature) with a 20-km crustal column (temperature obtained from parameterized convection model, as described by Phillips and Hansen [1998]), and accounting for the latent heat of the freezing magma. The height of the magma column derives from an isostatic assumption and an assumed 2-km plateau height but is consistent with the amount of partial melt that would be generated in the plume head. The resulting temperature profile was employed in the calculation of a yield stress envelope [*Brace and Kohlstedt*, 1980] for the development of tensile fractures and shear fractures using a Griffith failure criterion and a tensile yield stress, σ_0, of 12 MPa [*Jaeger and Cook*, 1979; *Sibson*, 1990]. The transition depth for tensile to shear failure is dependent on the choice of σ_0, and the 12 MPa value used is within the range estimated for intact basalt [*Schultz*, 1993]. The ductile portion of the curve derives from a flow law for Columbia diabase [*Mackwell et al.*, 1998]. Figure 11 shows the time it takes for the BDT in the

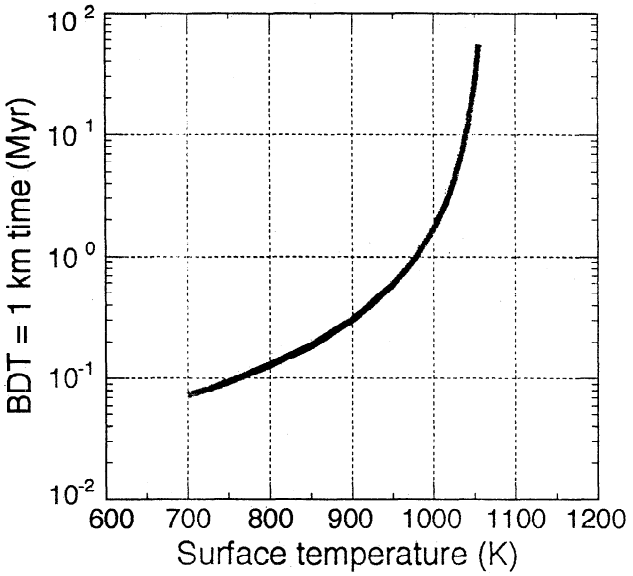

Figure 11. The time required for the brittle-ductile transition to migrate to a depth of 1 km as a function of surface temperature in a partially magmatized crust. Strength envelope is based on Griffith criterion for tensile and shear failure with a tensile strength of 12 MPa, which places the tensile-to-shear failure boundary at 1 km. Flow law is based on dry diabase. Half-space cooling model is employed with an initial temperature of mixed magma/crustal column, and a thermal diffusivity of 5×10^{-7} m^2 s^{-1}, consistent with the high temperature environment [*Hofmeister*, 1999]. These times could be substantially increased by the presence of partial melt and its effect on creep strength [*Kohlstedt and Chopra*, 1994].

cooling crustal column to reach a depth of 1 km as a function of surface temperature. Our choice of σ_0 also places the transition depth from tensile to shear fractures at 1 km, so this plot also gives approximately the time interval over which tensile fractures would develop because implied BDT depths for tensile ribbons do not generally exceed this depth [*Hansen and Willis*, 1998]. The surface temperature range used is 700 K to about 1050 K, which has a corresponding range of times from ~70,000 years to ~50 Myr. Geologically reasonable time periods (~1 Myr) for ribbon formation require surface temperatures in the range 900-1000 K.

The mixed crust-magma cooling model can be invoked to remove pre-ribbon craters within crustal plateaus by rapid viscous relaxation in the hot crustal environment. However, as the crust cooled with time, impact craters would be preserved; the cooling must proceed rapidly enough to create a sharp transition to the present suite of unrelaxed tessera craters. The crater retention age recorded on a crustal plateau is younger than the initiation age of the plateau by the time it takes the upper crust to strengthen. Using a model surface temperature of 740 K, in ~20 Myr the smallest 80% of the craters (≤30 km diameter) in the observed global size range could be supported by the strength of the crustal plateau crust. This result was obtained by constructing a yield strength envelope with a dry diabase flow law and considering a viscous yield strength of 50 MPa; in 20 Myr, this yield strength reached 15 km depth. Stresses imparted by a crater fall off with depth z approximately as $\exp[-(2\pi/\lambda)z]$ where λ is the effective wavelength of the crater (taken as the crater diameter). The support depth is taken as $z = \lambda/2$, since $\exp[-\pi] = 0.04$. Thus craters <30 km in diameter can be supported after ~20 Myr. The average global cratering rate can be obtained by the average crater retention age (~750 Myr [*McKinnon et al.*, 1997]) divided into the number of craters observed globally. From this we find that over a 20-Myr interval, the expected number of craters in this size range that would form (and thus be captured in a transitional state of relaxation/deformation, as implied by *Gilmore et al.* [1998]) on the largest of the crustal plateaus is only ~0.2. Larger (rarer) craters might be caught in transition as the strength boundary takes longer to deepen to the appropriate level, but the probabilities become exceedingly small. For a 900 K surface temperature, it takes ~70 Myr for the viscous yield strength to reach the depth required to support the smallest 80% of the crater population, and the expected number of craters is still less than one. Because the strength boundary depths for the formation of ribbons (~1 km) and folds (~6 km) are <15 km, these tectonic features would have formed within the transition interval from relaxed to unrelaxed craters. Thus the probability of creating a ribbon- or fold-deformed crater would seem to be exceedingly small. Thus we reject the assertion by *Gilmore et al.* [1998] that the hotspot model requires a range of crater deformation states.

4.2. Atmospheric changes over time

Gilmore et al.'s [1998] analysis also demonstrates misunderstanding of other aspects of the geodynamical model that evolved from the new hotspot model. *Phillips and Hansen* [1998] examined implications of the new hotspot model for the geodynamical evolution of Venus. (1) Thermomechanical modeling of ribbon formation indicates that the surface temperature might have been elevated (relative to present-day values) during ribbon formation in order to allow a geologically reasonable time period for tensile fracture ribbons to form (Figure 11). Other workers [*Solomon et al.*, 1998] have independently proposed elevated surface temperature to explain specific tectonic features on the planet. (2) The cause of elevated surface temperature of *Phillips and Hansen* [1998] is a great increase in volcanic greenhouse gases related to emplacement of massive volcanic plains; the plumes responsible for crustal plateau thickening were not proposed to cause elevated surface temperature as stated by *Gilmore et al.* [1998].

Gilmore et al. [1998, p. 16,836] pointed out that the 1000 K surface temperature used by *Phillips and Hansen* [1998] was "far above the temperature excursion modeled by *Bullock and Grinspoon* [1998] for a global volcanic event." *Bullock and Grinspoon* [1998, 2000] have presented models of volcanic outgassing on Venus that produce greenhouse surface temperatures approaching 900 K. In this work, there is enough uncertainty in model parameter values (e.g., exospheric escape time of hydrogen, outgassing history, atmosphere/interior climatic coupling, and surface/atmosphere chemical reactions, to name four), that it is reasonable to examine a surface temperature range up to at least 1000 K, where the time for the BDT to reach a 1-km depth is ~2 Myr (Figure 11). For 900 K the time is 0.3 Myr. *Phillips and Hansen* [1998, p. 1496] proposed that a 1000 K surface temperature would delay the onset of shear fracture ribbons for 1 Myr and pointed out that this "...approaches the duration of large terrestrial flood basalt events." This was only suggestive, and nowhere did they imply, or otherwise demonstrate, that this corresponded to the duration of ancient plume events on Venus.

Gilmore et al. [1998] also concluded erroneously that *Phillips and Hansen* [1998] assumed that plumes were the source of volatile outgassing to raise the greenhouse surface temperature, and then proceeded to dismantle the ribbons-form-over-plume argument in two ways: (1) The delay in the rise of surface temperatures following plume outgassing, due to the formation of massive (but transient) sulfuric acid/water clouds, would lead to implausible timing for ribbon formation. (2) Without the plume to enhance the greenhouse, an ad hoc global event at exactly the right time would be required. In fact, *Phillips and Hansen* [1998] invoked neither mechanism as a volatile source to enhance the greenhouse. *Phillips and Hansen* [1998, p. 1495] appealed to a continuous eruption of volcanic plains and stated: "During the formation of the voluminous plains, outgassing of volatiles should have enhanced the atmospheric greenhouse of Venus and thereby increased the surface temperature."

The thermal gradient inferences of *Gilmore et al.* [1998, Figure 21] are not relevant to the model of *Phillips and Hansen* [1998]. They are based on steady state heat flow, whereas *Phillips and Hansen* [1998] models imply transient cooling from a partially magmatized crust. For example, with a surface temperature of 900 K and a strain rate of 10^{-15} s^{-1}, *Phillips and Hansen* [1998] find that upon cooling, a BDT depth of 50 m is reached in 500 years. If we consider that some of the ribbons formed in a cooling lava pile, then a Stefan model [*Turcotte and Schubert*, 1982] increases the time to 2000 years.

5. Summary

Analysis of Magellan data indicates that there is no evidence to suggest that tesserae form a global onionskin on Venus, although ribbon-bearing tesserae reflect an ancient time of globally thin lithosphere. Individual tracts of ribbon-bearing tessera terrain did not form synchronously but rather punctuated time and space as individual deep mantle plumes imparted a distinctive rheological and structural signature on ancient thin crust across discrete 1600-2500 km diameter regions. Plume-related magmatic accretion led to crustal thickening at crustal plateaus. The surfaces of crustal plateaus record widespread early extension and local, minor perpendicular contraction of a thin, competent layer above a ductile substrate. This distinctive crustal rheology extended across individual crustal plateaus. As the depth to BDT increased with time, broad, gentle folds formed along plateau margins and short, variably oriented folds formed in the interior; local extension formed late complex graben. Local lava flows accompanied all stages of ribbon, fold, and complex graben formation. Geodynamical models that build on or incorporate ribbon-bearing tesserae or crustal plateau relations as fundamental assumptions or constraints must take these findings into account.

Gilmore et al.'s [1998] attempt to discount structural and kinematic analyses of ribbon structures, and implications of ribbon structures for crustal plateau evolution and Venus geodynamical models, is unfounded. Problems with *Gilmore et al.'s* [1998] analysis range from incorrect methodology to misunderstanding the models that they proposed to test. *Gilmore et al.* [1998] did not differentiate ribbons from graben; they disregarded shear fracture ribbons; they misrepresented previous radargrammetric work that constrains ribbon geometry; they used solely geometrical relations in attempts to constrain structural temporal relations in violation of kinematic analysis; and their attempts to place stratigraphic constraints on ribbon-fold temporal relations are invalid. *Gilmore et al.'s* [1998] attempts to discount models of crustal plateau formation fail in that they did not differentiate between fundamentally different pre-Magellan and post-Magellan upwelling models. They have illustrated several misconceptions about the new upwelling model and processes responsible for global warming, which lead to serious errors in their criticism. In light of these errors, the analysis of *Gilmore et al.* [1998] presents no robust scientific challenge to the upwelling model of crustal plateau formation of any of its building blocks. The new data and interpretations presented here lend further support to previous interpretations and indicate that tessera terrain is not globally distributed in time or space.

Acknowledgments. This work was supported by NASA's Planetary Geology and Geophysics programs under grants NAGW-2915 and NAG5-4562 to Southern Methodist University and NAG5-4448 to Washington University. We thank Bruce Campbell and Ellen Stofan for review comments; Campbell provided a particularly thorough review.

References

Angelier, J., F. Bergerat, and T. Villemin, Effective tension-shear relationships in extensional fissure swarms, axial rift zone of northeastern Iceland, *J. Struct. Geol.*, *19*, 673-685, 1997.

Baldwin, R. B., Rima Golcenius II, *J. Geophys. Res.*, *76*, 8459-8465, 1971.

Banks, B. K., and V. L. Hansen, Crustal plateau intra-tessera flood lava basins, Venus, *Geol. Soc. Am. Abstr.* Programs, *30*, A190, 1998.

Banks, B. K., and V. L. Hansen, Intratessera flood-lava basins (ITBs) constrain timing of crustal plateau structures, *Lunar Planet. Sci.* [CD-ROM], *XXX*, Abstract 2053, 1999.

Basilevsky, A. T., and J. W. Head, The geologic history of Venus: A stratigraphic view, *J. Geophys. Res.*, *103*, 8531-8544, 1998.

Basilevsky, A. T., A. A. Pronin, L. B. Ronca, V. P. Kryuchkov, A. L. Sukhanov, and M. S. Markov, Styles of tectonic deformations on Venus: Analysis of Venera 15 and 16 data, *Proc. Linar Planet. Sci. Conf., 16th*, Part 2, *J. Geophys. Res.*, *91*, suppl., D399-D411, 1986.

Bindschadler, D. L., Magellan—A new view of Venus geology and geophysics, *Rev. Geophysics*, *33*, 459-467, 1995.

Bindschadler, D. L., and E. M. Parmentier, Mantle flow tectonics: The influence of a ductile lower crust and implications for the formation of topographic uplands on Venus, *J. Geophys. Res.*, *95*, 21329-21344, 1990.

Bindschadler, D. L., G. Schubert, and W. M. Kaula, Coldspots and hotspots: Global tectonics and mantle dynamic of Venus, *J. Geophys. Res.*, *97*, 13495-13532, 1992a.

Bindschadler, D. L., A. deCharon, K. K. Beratan, and J. W. Head, Magellan observations of Alpha Regio: Implications for formation of complex ridged terrains on Venus, *J. Geophys. Res.*, *97*, 13,563-13,577, 1992b.

Brace, W. F., and D. L. Kohlstedt, Limits on lithospheric stress imposed by laboratory experiments, *J. Geophys. Res.*, *85*, 6248-6252, 1980.

Brown, C. D., and R. E. Grimm, Tessera deformation and the contemporaneous thermal state of the plateau highlands, Venus, *Earth Planet. Sci. Lett.*, *147*, 1-10, 1997.

Bullock, M. A., and D. H. Grinspoon, Geological forcing of surface temperatures on Venus, *Lunar Planet. Sci.* [CD-ROM], *XXIX*, Abstract 1542, 1998.

Bullock, M. A., and D. H. Grinspoon, The recent climate evolution of Venus, *Icarus*, in press, 2000.

Coffin, M. F., and O. Eldholm, Large igneous provinces: Crustal structure, dimensions, and external consequences, *Rev. Geophys.*, *32*, 1-36, 1994.

Davis, G. H., and S. J. Reynolds, *Structural Geology of Rocks and Regions*, John Wiley, New York, 1996.

Farnetani, C. G., and M. A. Richards, Numerical investigations of the mantle plume initiation model for flood basalt events, *J. Geophys. Res.*, *99*, 13813-13833, 1994.

Ford, J. P., J. J. Plaut, C. M. Weitz, T. G. Farr, D. A. Senske, E. R. Stofan, G. Michaels and T. J. Parker, *Guide to Magellan Image Interpretation*, JPL Publ., 93-24, 1993.

Ghent, R. R. and V. L. Hansen, Structural analysis of eastern and central Ovda Regio, Venus: Implications for crustal plateau formation, *Icarus*, *139*, 116-136, 1999.

Gilmore, M. S., M. I. Ivanov, J. Head, and A. Basilevsky, Duration of

tessera deformation on Venus, *J. Geophys. Res.*, *102*, 13,357-13,368, 1997.

Gilmore, M. S., G. C. Collins, M. A. Ivanov, L. Marinangeli, and J. W. Head, Style and sequence of extensional structures in tessera terrain, Venus, *J. Geophys. Res.*, *103*, 16,813-16,840, 1998.

Golombek, M. P., Structural analysis of lunar grabens and the shallow crustal structure of the moon, *J. Geophys. Res.*, *84*, 4657-4666, 1979.

Griffiths, R. W., and I. H. Campbell, Interaction of mantle plume heads with the Earth's surface and onset of small-scale convection, *J. Geophys. Res.*, *96*, 18,295-18,310, 1991.

Grimm, R. E., Recent deformation rates on Venus, *J. Geophys. Res.*, *99*, 23,163-23,171, 1994a.

Grimm, R. E., The deep structure of venusian platcau highlands, *Icarus*, *112*, 89-103, 1994b.

Hansen, V. L., and J. J. Willis, Structural analysis of a sampling of tesserae: Implications for Venus geodynamics, *Icarus*, *123*, 296-312, 1996.

Hansen, V. L. and J. J. Willis, Ribbon terrain formation, southwestern Fortuna Tessera, Venus: Implications for lithosphere evolution, *Icarus*, *132*, 321-343, 1998.

Hansen, V. L., J. J. Willis, and W. B. Banerdt, Tectonic overview and synthesis, in *Venus II*, edited by S. W. Bouger, D. M. Hunten, and R. J. Phillips, pp. 797-844, Ariz. Univ. Press, Tucson, 1997.

Hansen, V. L., B. K. Banks, and R. R. Ghent, Tessera terrain and crustal plateaus, Venus, *Geology, 27*, 1071-1074, 1999.

Head, J. W., Tectonic facies in Venus tessera terrain: Classification and interpretation of sequence of deformation (abstract), *Lunar Planet. Sci., XXVI*, 579-580, 1995.

Head, J. W., and A. T. Basilevsky, Sequence of tectonic deformation in the history of Venus: Evidence from global stratigraphic relations, *Geology, 26*, 35-38, 1998.

Herrick, R. R., Resurfacing history of Venus, *Geology, 22*, 703-706, 1994.

Herrick, R. R., and R. J. Phillips, Blob tectonics: A prediction for western Aphrodite Terra, Venus, *Geophys. Res. Lett.*, *17*, 212-2132, 1990.

Hofmeister, A. M., Mantle values of thermal conductivity and a geotherm from phonon lifetimes, *Science, 283*, 1699-1706, 1999.

Hudleston, P., and L. Lan, Rheological information from geological structures, *Pure Appl. Geophys.*, *145*, 607-620, 1995.

Ivanov, M. A., and J. W. Head, Tessera terrain on Venus: A survey of the global distribution, characteristics, and relation to surrounding units from Magellan data, *J. Geophys. Res.*, *101*, 14,861-14,908, 1996.

Ivanov, M. A., and J. W. Head, Ridge-ribbon age relationships in northeast Ovda Regio, Venus, *Lunar Planet. Sci.* [CD-ROM], *XXX*, Abstract 1232, 1999.

Jaeger, J. C., and N. G. W. Cook, *Fundamentals of Rock Mechanics*, Chapman and Hall, New York, 1979.

Kidder, J. G., and R. J. Phillips, Convection-driven subsolidous crustal thickening on Venus, *J. Geophys. Res.*, *101*, 23,181-23,194, 1996.

Kohlstedt, D. L., and P. N. Chopra, Influence of basaltic melt on the creep of polycrystalline olivine under hydrous conditions, in *Magmatic Systems*, edited by M. P. Ryan, pp. 37-53, Academic, San Diego, Calif., 1994.

Lloyd, G. E., and C. C. Fergusson, Boudinage structure: Some interpretations based on elastic-plastic finite element simulations, *J. Struct. Geol.*, *3*, 117-128, 1981.

Lloyd, G. E., C. C. Fergusson, and K. Reading, A stress transfer model for the development of extension fracture boudinage, *J. Struct. Geol.*, *4*, 355-372, 1982.

Mackwell, S. J., M. E. Zimmerman, and D. L. Kohlstedt, High-temperature deformation of dry diabase with application to tectonics on Venus, *J. Geophys. Res.*, *103*, 975-984, 1998.

Mankin, J. H., The down-structure method of viewing geologic maps, *J. Geol.*, *58*, 55-72, 1950.

McGill, G. E., Attitude of fractures bounding straight and arcuate lunar rilles, *Icarus*, *14*, 53-58, 1971.

McGill, G. E., and A. W. Stromquist, The grabens of Canyonlands National Park, Utah: Geometry, mechanics and kinematics, *J. Geophys. Res.*, *84*, 4547-4563, 1979.

McKinnon, W. B., K. J. Zahnle, B. A. Ivanov, and H. J. Melosh, Cratering on Venus: Models and observations, in *Venus II*, edited by S. W. Bouger, D. M. Hunten, and R. J. Phillips, pp. 969-1014, Univ. of Ariz. Press, Tucson, 1997.

Nimmo, F., and D. McKenzie, Volcanism and tectonics on Venus, *Annu. Rev. Earth Planet. Sci.*, *26*, 23-52, 1998.

Phillips, R. J., and V. L. Hansen, Tectonic and magmatic evolution of Venus, *Annu. Rev. Earth Planet. Sci.*, *22*, 597-654, 1994.

Phillips, R. J., and V. L. Hansen, Geological evolution of Venus: Rises, plains, plumes and plateaus, *Science*, *279*, 1492-1497, 1998.

Phillips, R. J., R. E. Grimm, and M. C. Malin, Hot-spot evolution and the global tectonics of Venus, *Science*, *252*, 651-658, 1991.

Plaut, J. J., Stereo imaging, in *Guide to Magellan Image Interpretation*, edited by J. P. Ford et al., *JPL Publ., 93-24*, 33-41, 1993.

Price, N., and J. Cosgrove, *Analysis of Geological Structures*, Cambridge Univ. Press, New York, 1990.

Pritchard, M. E., V. L. Hansen, and J. J. Willis, Structural evolution of western Fortuna Tessera, Venus, *Geophys. Res. Lett.*, *24*, 2339-2342, 1997.

Ramberg, H., Natural and experimental boudinage and pinch-and-swell structures, *J. Geol.*, *63*, 512-526, 1955.

Ramsay, J. G., and M. I. Huber, *The Techniques of Modern Structural Analysis: Strain Analysis*, Academic, San Diego, Calif., 1983.

Ramsay, J. G., and M. I. Huber, *The Techniques of Modern Structural Analysis: Folds and Fractures*, Academic, San Diego, Calif., 1987.

Saunders, R. S., et al., Magellan mission summary, *J. Geophys. Res.*, *97*, 13,063-13,066, 1992.

Schultz, R., Brittle strength of basaltic rock masses with applications to Venus, *J. Geophys. Res.*, *98*, 10,833-10,895, 1993.

Sibson, R. H., Conditions for fault-valve behavior, in *Deformation mechanisms, Rheology and Tectonics*, edited by R. J. Knipe and E. H. Rutter, pp. 15-28, Geol. Soc., London, 1990.

Simons, M., S. C. Solomon, and B. H. Hager, Localization of gravity and topography: constraints on the tectonics and mantle dynamics of Venus, *Geophys. J. Int.*, *131*, 24-44, 1997.

Smrekar, S. E., and R. J. Phillips, Venusian highlands: Geoid to topography ratios and their implications, *Earth Planet. Sci. Lett.*, *107*, 582-597, 1991.

Smith, W. H. F., and D. T. Sandwell, Global sea floor topography from satellite altimetry and ship depth soundings, *Science, 277*, 1956-1962, 1997.

Solomon, S. C., The geophysics of Venus, *Phys. Today, 46/47*, 48-55, 1993.

Solomon, S. C., J. W. Head, W. M. Kaula, D. McKenzie, B. Parsons, R. J. Phillips, G. Schubert, and M. Talwani, Venus tectonics: Initial analysis from Magellan, *Science, 252*, 297-312, 1991.

Solomon, S. C, M. A. Bullock, and D. H. Grinspoon, Climate change as a regulator of global tectonics on Venus, *Lunar Planet. Sci.* [CD-ROM], *XXIX*, Abstract 1624, 1999.

Strom, R. G., G. G. Schaber and D. D. Dawson, The global resurfacing of Venus, *Journal of Geophysical Research*, *99*, 10,899-10,926, 1994.

Turcotte, D. L., An episodic hypothesis for Venusian tectonics, *J. Geophys. Res.*, *98*, 17,061-17,068, 1993.

Turcotte, D. L., and G. Schubert, *Geodynamics: Applications of Continuum Physics to Geological Problems*, John Wiley, New York, 1982.

Twiss, R. J., and E. M. Moores, *Structural Geology*, W.H. Freeman, New York, 1992.

van der Pluijm, B. A., and S. Marshak, *Earth Structure: An Introduction to Structural Geology and Tectonics*, McGraw-Hill, New York, 1997.

Watkinson, A. J., Fold propagation and interference in a single multilayer unit, *Tectonophysics*, *34*, T37-T42, 1976.

Watkinson, A. J., Patterns and strain influenced by linearly anisotropic bands, *J. Struct. Geol.*, *5*, 449-454, 1983.

Watts, A. B., and U. S. ten Brink, Crustal structure, flexure, and subsidence history of the Hawaiian Islands, *J. Geophys. Res.*, *94*, 10,473-10,500, 1989.

Zuber, M. T., Constraints on the lithospheric structure of Venus from mechanical models and tectonic surface features, *Proc. Linar Planet. Sci. Conf., 17th*, Part 2, *J. Geophys. Res.*, *92*, suppl., E541-E551, 1987.

R. R. Ghent, and V. L. Hansen, Department of Geological Sciences, Southern Methodist University, 2335 Daniel Avenue, Dallas, TX 75275-0395. (rghent@mail.smu.edu;vhansen@mail.smu.edu.)

R. J. Phillips, Department of Earth and Planetary Sciences, Washington University, Campus Box 11169, 1 Brookings Drive, St. Louis, MO 63130-4899. (phillips@wustite.wustl.edu.)

J. J. Willis, Department of Geology, University of Louisiana at Lafayette, Lafayette, LA 70504. (jjw9440@usl.edu.)

(Received July 8, 1999; revised November 16, 1999; accepted December 7, 1999.)